8

Gas-Liquid Mass Transfer in Gassed Mechanically Agitated Vessels

In the gas-liquid contactor, the mass transfer between gas and liquid through their interface is often the rate-controlling step, which always closely related the performance of the process result. In this chapter, the most important rate coefficient ”liquid-side mass transfer coefficient” in the transfer process of the gas-liquid contactors will be examined thoroughly. The experimental results obtained from single impeller systems will be used to discuss the effects of impeller type and number and size of blades on the value of K_La. The effect of gas recirculation around each impeller also to be examined to see how the amount of recirculated gas will affect the rate of local mass transfer. These results would be extended to multiple impeller system with various impeller combinations, i.e. the RRR, PRR, PPR and PPP systems, and procedures for predicting mass transfer characteristics of any given multiple impeller system will be presented.

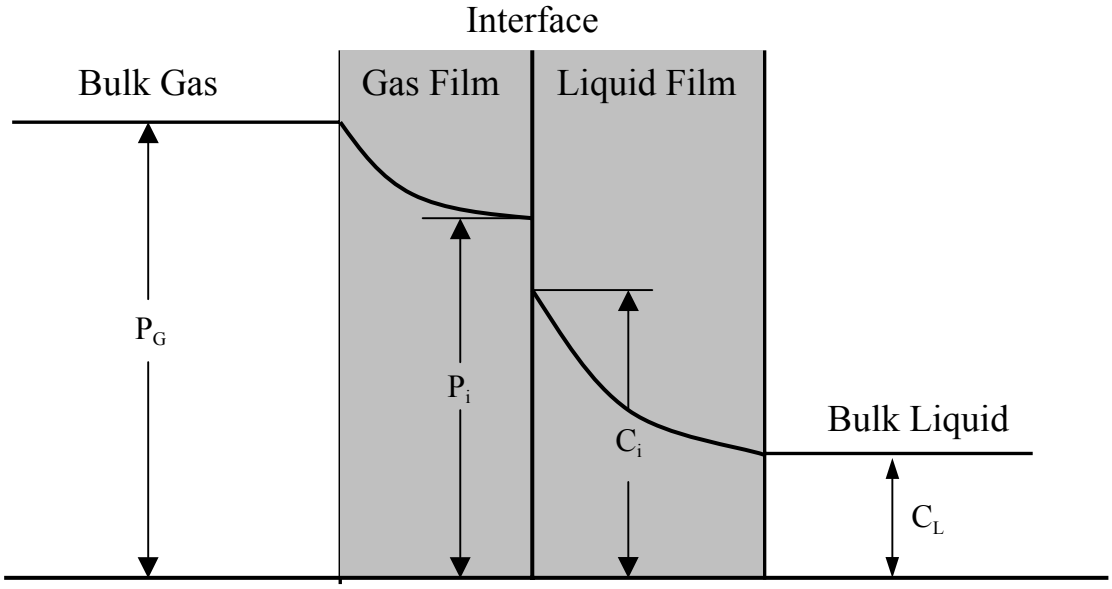

Fig. 8.1-1 The concentration profile of the transfer substance at each layer in transfer process at gas and liquid interface.

8.1 Mass Transfer Mechanism between Liquid and Gas Phases

Figure 8.1-1 illustrates the transfer steps from the gas phase to liquid phase. The whole process includes several steps, i.e.(1) conveying the solute gas from bulk gas to gas film;(2) diffusion of the solute gas through gas film to interface;(3)cross over interface according its equilibrium relationship;(4) diffusion of the solute through liquid film to the edge of bulk liquid;(5) conveying the solute by turbulent diffusion to bulk liquid. The concentration of the transferring substance at each layer is also shown in this figure. Where C_G, $C_{Gi,}$ C_e and C_L denotes the solute concentration in the gas phase, gas-liquid interface, the equilibrium dissolved solute concentration at liquid film in respect to gas film and liquid phase, respectively.

In the gas-liquid mechanically agitated systems, the mass transfer processes from gas to bulk liquid are usually the rate-determining step. From the film theory, it is acknowledged that two mass transfer coefficients, the **gas side coefficient k_Ga** and the **liquid side coefficient, K_La,** exist at the interface. The rate of mass transfer, N, (Kg-mole/sec) is proportional to area of interface, a[m^2/m^3] and concentration difference between two phases, ΔC[kg-mole/m^3], or

$$N = \frac{dw}{dt} = KaV\Delta C \tag{8.1-1}$$

where K is a proportional constant, which is known as **mass transfer coefficient** [m/sec] and V is the liquid volume. The mass transfer rate can be also expressed as

$$N = k_L aV(C_i - C_L) \tag{8.1-2}$$

$$N = k_G aV(P_G - P_i) \tag{8.1-3}$$

Since it is quite difficult to determine the value of C_i or P_i accurately, the corresponding equilibrium pressure P^* and liquid concentration C* are adopted to rewrite the Eqs. (8.1-2) and (8.1-3) as

$$N = K_L aV(C^* - C_L) \tag{8.1-4}$$

and

$$N = K_G aV(P_G - P^*) \tag{8.1-5}$$

$K_L$ais known as liquid-side volumetric mass transfer coefficient and K_Ga is known as gas-side volumetric mass transfer coefficient. Integration of Eq. (8.1-4) will give

$$K_L aV = \frac{1}{t_1 - t_2} \ln \frac{C^* - C_1}{C^* - C_2} \tag{8.1-6}$$

This expression can be used to determine the value of K_La if bulk concentration of C and the corresponding equilibrium concentration C* at a time interval are known. Since the value of

interfacial area is difficult to estimate, the mass transfer characteristic is often expressed in terms of $\mathbf{K_L a}$ or $\mathbf{K_G a}$.

Since the diffusivities in the gas phase is high and the viscosity of gas is much lower than that of liquid, the mass transfer resistance in the gas phase can be considered negligible. Hence, the **liquid side volumetric mass transfer coefficient $\mathbf{K_L a}$** becomes the most dominant factor in the entire transport process within the mechanically agitated vessel. It contains both the mass transfer coefficient $\mathbf{K_L}$ and the interfacial area **a**. K_L is mainly dependent on the properties and hydrodynamics of the liquid. However, the interfacial area a is dependent on the amount of gas hold up and bubble sizes in the agitated vessel, which are determined by the flow field, power consumption and gas dispersing characteristic of the impeller, etc.

Table 8.1-1 Methods for measuring the liquid volumetric mass transfer coefficient.

Chemical Methods
1. Sulfite Method (Copper, 1944) 2. Glucose Oxidase Method (Hsieh, 1969) 3. Carbon Dioxide Absorption Method (Lee, 1982) 4. Hydrogen Peroxide Method (Hickman, 1988)
Physical Methods
Steady State Approaches 1. Mass Balance Method (Chain, 1966) 2. Steady State Method for Continuous flow (Greaves, 1985) **Dynamic Methods** 1. $\mathbf{N_2}$ Gassing out Method (Wize, 1951) 2. Original Dynamic Method (Humphrey, 1967) a. For Low Cell Concentration System b. For High Cell Concentration System 3. Modified $\mathbf{N_2}$ Gassing out Method (Heineken,1970, etc.) 4. Modified Dynamic Method (Aiba, 1984, etc.) 5. Dynamic Pressure Method (Linek, 1989) 6. Gassing-in with 02-Enriched Air Method (Moo-Young, 1989)

8.1.1 Methods of determining $K_L a$

The methods to determine the value of $K_L a$ can be classified into two categories: (1) chemical methods and (2) physical methods. Chemical methods are based on the

determination of absorption rate per unit interfacial area, which can be evaluated from the theory of gas absorption with chemical reaction in the liquid phase. Interfacial area can then be calculated from measurement of the absorption rates. For fast chemical reactions, the absorption rate is determined by the chemical reaction only and not by the physical absorption. The reactions are selected to be fast and the rate of absorption is independent of K_L and the hydrodynamic conditions. However, two major difficulties come with the chemical methods: (1) The requirement of the kinetics of the reaction diminishes the application of the chemical methods: (2) The influence of reactants (e.g.: Sodium Sulfite) on the properties of the reacting system confines the application of chemical methods to the system without reaction. In comparison with the chemical methods, the physical methods can estimate K_La from gas absorption data without chemical reaction. Such methods are independent on the rate of the reaction and can be applied to the system with or without reaction. In all existed methods, the physical and the steady-state reaction methods are more popular for the determination of K_La. Table 8.1-1 lists the measuring methods, which were used by the previous researchers.

8.1.2 Previous Correlations of K_La

For mechanically agitated gas-liquid contactors, straight blade disk turbines have been adopted because of its superiority dispersing gas into liquid. A number of correlations have been proposed for estimating K_La in gassed vessels equipped with disk turbine impellers, mostly for Rushton turbine impeller. Table 8.1-2(a) and (b) list such correlations for non-ionic and ionic systems respectively. Although some correlations seem to be incompatible with each other, the correlations always showed that the mass transfer coefficient was a function of power consumption per unit volume and superficial gas velocity no matter what measuring methods were adopted. However these correlations consider only the rate of sparging gas to the impeller as the main parameter and neglect the effects of the gas recirculation around the impeller, which may mislead the results of analysis. From the experimental and the simulated results, it was shown that the gas recirculation rate has a great influence on the power drawn by the impeller and affects mass transfer rate pronouncedly. For the multiple impeller systems, because of the non-uniform gas loading over impellers, the gas recirculation rate and the mass transfer rates in each impeller regions is quite different from each other. Using the total gassing rate (i.e. the sum of recirculation rate plus gas sparging rate) to replace the gas sparging rate impeller to correlate K_La can grasp a more correct understanding about the mass transfer phenomenon between gas and liquid in a mechanically stirred vessel.

Table 8.1-2 List of the previous correlations of K_La.

(a) Non-ionic System

Investigators	Vessel Diameter T(cm)	D/T	Correlations	Measuring methods
Rushton et al.(1956)	15.3, 30.6	0.33	$K_La \propto (P_g/V)^{0.71\text{-}0.79}(V_S)^{0.76}$	Sodium Sulfite
Koetsier et al.(1973)	19,60		$K_La \propto (P_g/V)^{0.65}(D/T)^{0.65}T^{-0.33}$	Chemical and Physical
Yagi and Yoshida (1975)	25	0.4	$K_La \propto (P_g/V)^{0.74}(V_S)^{0.28}$	Desorption of Oxygen
Smith et al. (1977)	0.61	0.33	$K_La \propto (P_g/V)^{0.475}(V_S)^{0.4}$	
Van't Riet et al. (1979)			$K_La \propto (P_g/V)^{0.4}(V_S)^{0.5}$	
Nishikawa et al. (1981)	15,20,30,60	0.3-0.5	$K_La \propto (P_g/V)^{0.8}(V_S)^{0.33}$	Sodium Sulfite
Greaves and Loh (1985)			$K_La \propto (P_g/V)^{0.4}(V_S)^{0.5}$	Steady state
Hickman (1988)	60,200	0.33	$K_La \propto (P_g/V)^{0.54}(V_S)^{0.68}$	Steady state H_2O_2

(b) Ionic System

Investigators	Vessel Diameter T(cm)	D/T	Correlations	Measuring methods
Koetsier et al. (1973)	19,60		$K_La \propto (P_g/V)^{0.7}(D/T)^{0.7}T^{-0.35}$	Chemical and Physical
Van't Riet et al. (1979)			$K_La \propto (P_g/V)^{0.7}(V_S)^{0.2}$	
Smith et al. (1977)	0.61	0.33	$K_La \propto (P_g/V)^{0.475}(V_S)^{0.4}$	

Up to this date, the most acknowledged correlation to estimate the value of K_La in a single impeller system is proposed by van't Riet, 1979 as:

$$K_La=0.026(P_g/V)^{0.4}V_S^{0.5} \quad T<2.6m \tag{8.2-1}$$

Figure 8.1-2 showed the correlation of van't Riet (1979) and the experimental data of the authors'. It can be found that the deviations between them were very small, which confirms the reliability of the correlation.

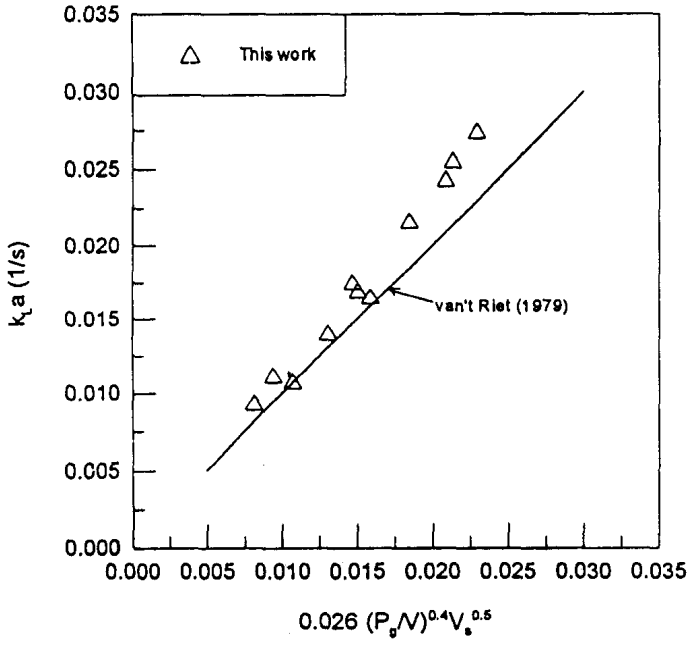

Fig. 8.1-2 Correlation of van't Riet (1979).

8.2 Mass Transfer Characteristics of Various Impellers in Single Impeller System

8.2.1 The Rushton turbine impeller

Since the value of K_La is a product of the gas-liquid interfacial area "a" and the liquid film transfer coefficient "$\mathbf{K_L}$" and the value of **a** is determined by bubble sizes and local gas hold-up which are mainly controlled by the performance of gas dispersion of the impeller while $\mathbf{K_L}$ depends on the local turbulent intensity, which is closely related to energy dissipation rate, therefore prior to grasp the mass transfer phenomenon in a gassed agitated vessel, one should know the hydrodynamics of the system.

Fig.8.2-1 depicts the liquid velocity distribution and local energy dissipation rate of the single Rushton Impeller system. It can be seen the lager values of velocity vectors and energy dissipation rates always appear in the discharge stream of the impeller and decrease significantly along the circulatory loop.

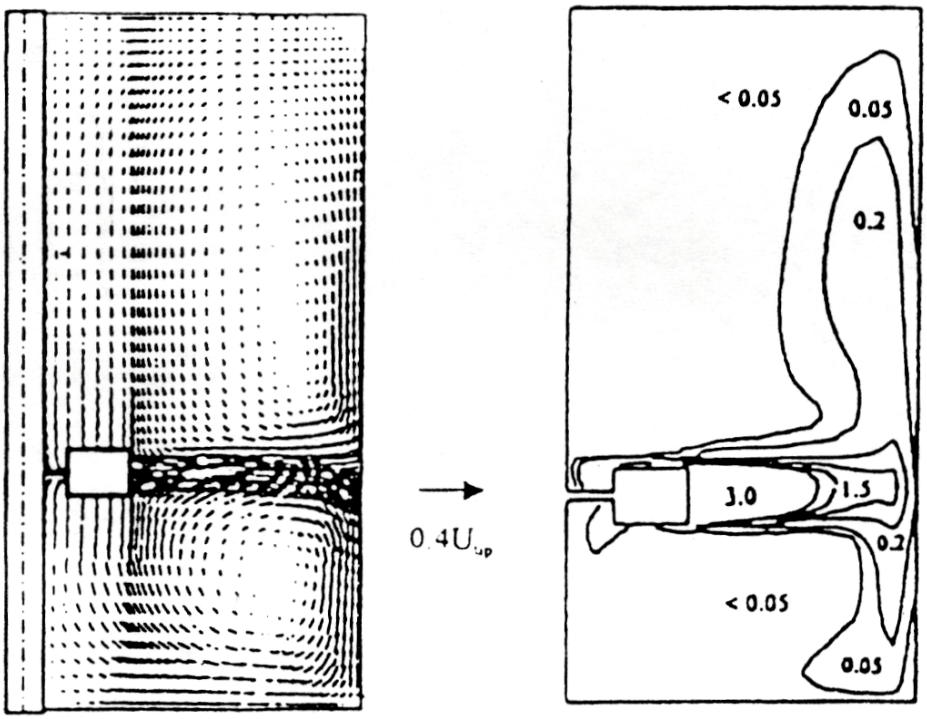

Fig. 8.2-1 Distribution of liquid velocity vector and local energy dissipation rate for a single Rushton turbine impeller system under N=13.3 rps and P_g/V=528.3W/m^3.

Effect of blade number of Rushton turbine impeller on the mass transfer rate

Contrast to the researches for a single standard Rushton turbine impeller(with six blades) system, there are only few research efforts on the other design disc turbine impellers on the gas dispersion and mass transfer. Lu and Yang (1995) had applied the LDV and modified

capillary method to measure the turbulent intensity and dispersed bubble size in the stirred vessel to examine the effects of the number of impeller blades on flow pattern and gas dispersion. By comparing the experimental data of a 2, 4-, 6-, 8-blades disk impeller, they pointed out that under a low gassing condition the turbulent intensity is strongest for the 4-blade impeller, and the dispersed bubbles are also the smallest. These results imply that the 4-blade impeller has the best gas dispersion capability and results in a better mass transfer rate. However, by comprising these results with the other previous works in the literatures, the almost contrary conclusions were obtained. To clarify this contradiction, the volume-averaged mass transfer coefficient of the systems equipped with impellers having different number of blades under various gassing rates were measured and were compared under three conditions, i.e. (1) with the same rotational speed; (2) with the same total power consumption (3) with the same power consumption per blade to estimate the effects of the blade number and aerate rates on the mass transfer rate. Figure 8.2-2 showed the overall averaged $<K_La>$ for the single 2-, 4-, 6-, 8-blade disk turbine impeller systems under the same rotational speed N=13.3 rps. From this figure, From these plots, two noticeable points can seen, (1) the $<K_La>$ value for each impeller always increased monotonically with the increase of gassing rates; (2) no matter what the gassing rate was, the impeller with more blades always dispersed the gas more effectively, which induce the higher value of $<K_La>$. However, under the same rotatioal speed the impeller having more blades always draws more power, which may not be economic for industrial processes. In Fig.8.2-3, the variations of $<K_La>$ for the impeller with 4, 6 and 8 blades with the same power consumption per unit liquid volume of P_g/V=559.36 W/m^3 under various gas flow rates are shown. It can be found that (1) with the same power consumption $<K_La>$ always increases with the increase in the gassing rates; (2) the 4-blade impeller under a low gassing rate condition(Q_S<0.5vvm) will have a higher $<K_La>$ than the 6-and 8- blade impellers, consistent with the results of Lu and Yang(1996). However, with the increase in gassing rates, the 6-blade impeller demonstrates stronger capability to disperse gas and the impeller having more blades performs better in gas dispersion. It is interesting to note that under a certain value of P_g/V the impeller equipped with 6 blades always gives a higher $<K_La>$ than that of the 8-blade impeller. In Fig. 8.2-4, the $<K_La>$ values for 4-, 6- and 8-blade impeller were compared under two different power consumption levels. From this figure, it can be seen that the $<K_La>$ values of the impeller with six blades always performs better in gas dispersion than the impellers with 4 and 8 blades.

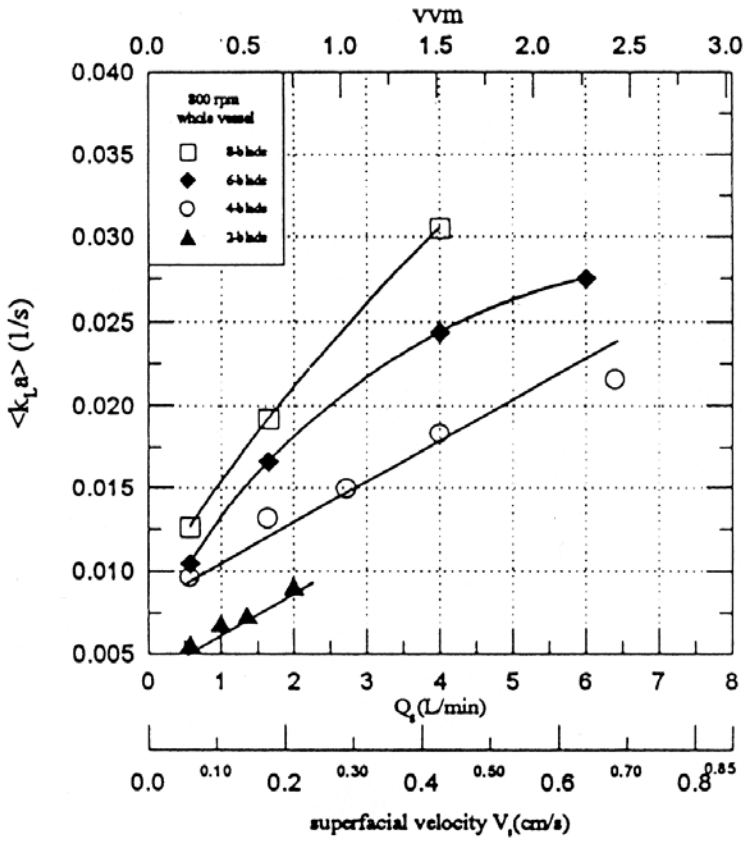

Fig. 8.2-2 Comparison of $<K_La>$ etween the single 2-, 4-, 6- and 8-blade disk turbine impeller systems with N=13.3rps.

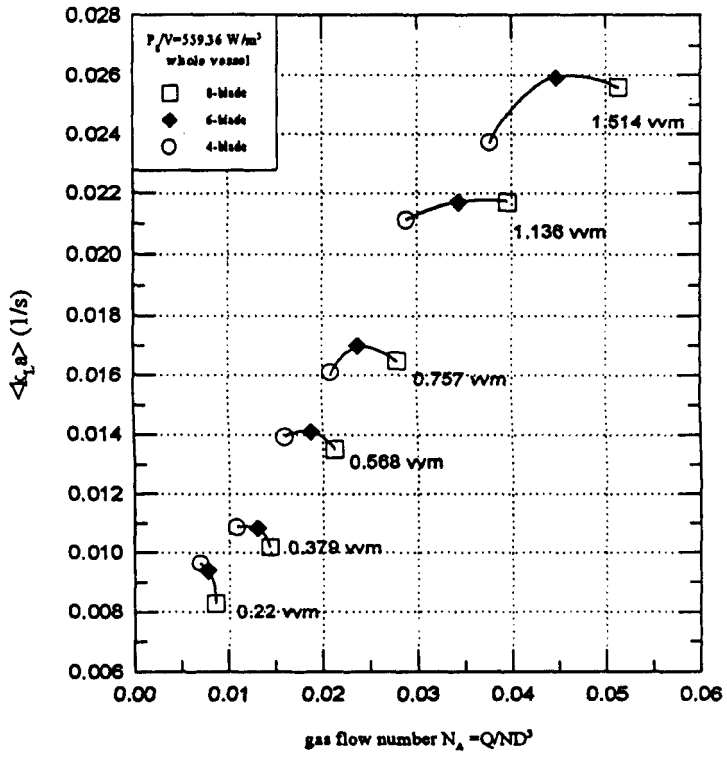

Fig. 8.2-3 Comparison of $<K_La>$ between the single 4-, 6- and 8-blade disk turbine impeller systems with $P_g/V=559.36W/m^3$.

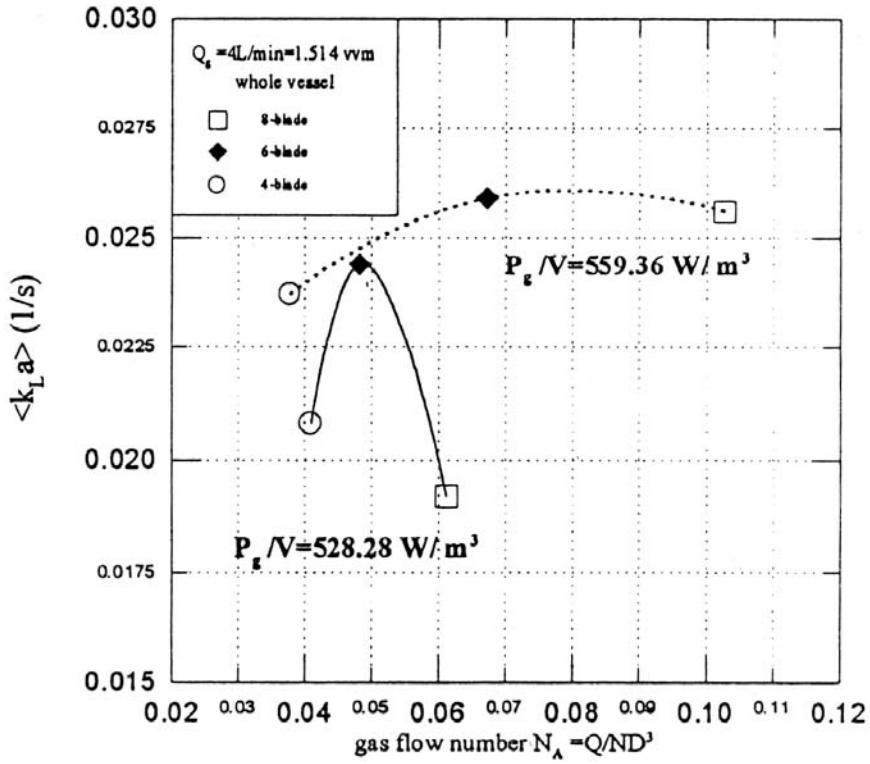

Fig. 8.2-4 Effect of power consumption level on <K_La> of the single 4-, 6- and 8-blade disk turbine impeller systems.

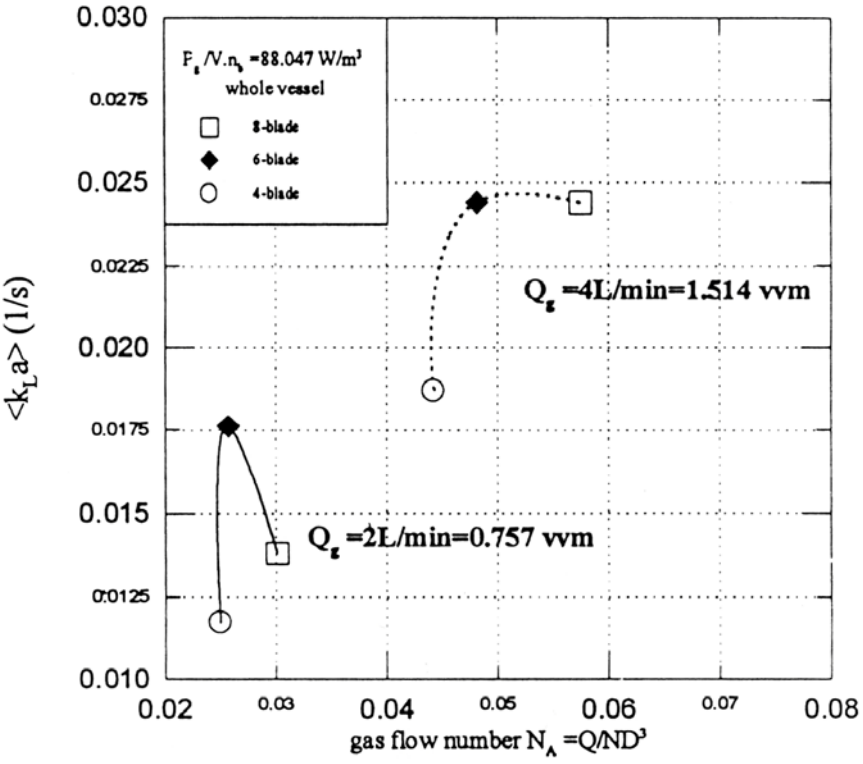

Fig. 8.2-5 Effect of impeller blade number and gas flow rate on <K_La> under the same power consumption per blade ($P_g/V \cdot n_b$=88.0W/m^3).

Figure 8.2-5 showed a comparison of the $<K_La>$ values for the 4- 6-, 8-blade impeller under two different gassing conditions with the same power consumption per blade ($P_g/V \cdot n_b$=88.0W/m^3). From this figure, it can be found that if the gassing rate is larger than 0.5vvm and does not exceed 1.6vvm(or m^3/s), the 6-blade impeller will perform better than the other impellers. The 8-blade impeller will become the prevailing one if the gassing rate exceeds this value.

From the above results, it can be clearly concluded that in the single impeller system the 4-blade impeller gives the best mass transfer performance only under a low aerated condition. Under the higher power input and gassing rate, the impeller with moor blades is more likely to have good gas dispersion or a higher value of K_La.

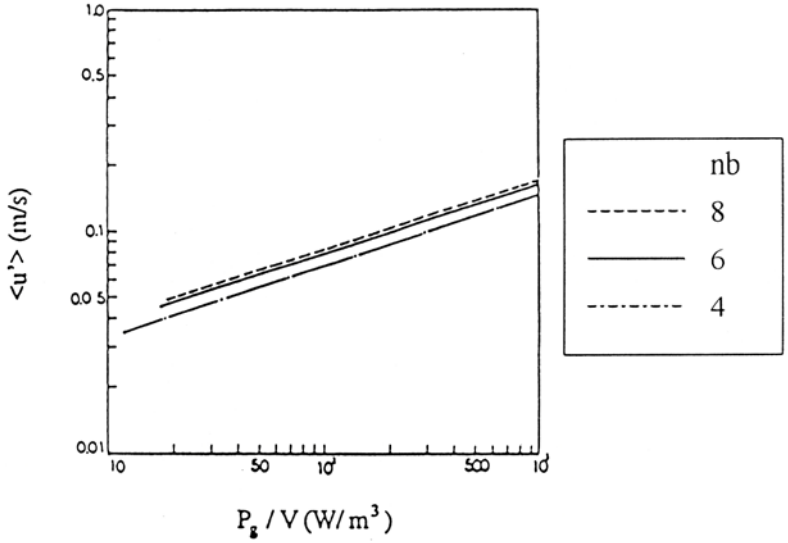

Fig. 8.2-6 Relationship between volume-average fluctuating velocity <u'> and P_g/V for the various blade number impeller.

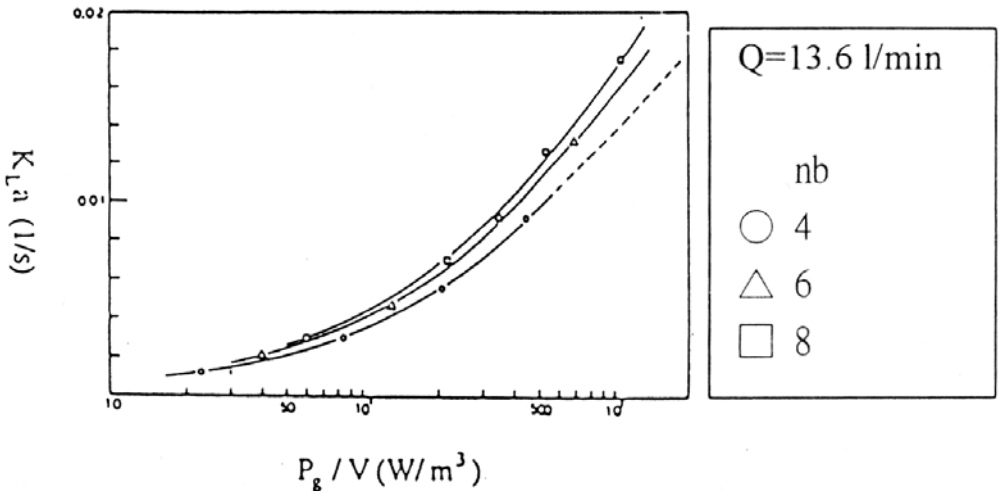

Fig. 8.2-7 Relationship between volume-average mass transfer coefficient $<K_La>$ and P_g/V for the various blade number impeller.

Relationship between Turbulent Fluctuating Velocity and Operating Variables

In Fig. 8.2-6, the effects of P_g/V on <u'> in the larger vessel for impellers having different numbers of blades are shown (Lu and Wu, 1988). The results clearly indicate that it is impossible to correlate <u'> with P_g/V using a single line if tile blade number of impeller is not the same or the type of impeller is different. Similar situation is also observed from the plot of $<K_La>$ vs. P_g/V for impellers having different blade number as shown in Fig. 8.2-7, which is not consistent with the results of the previous researches. These facts again point out that P_g/V is not always a good scale up basis (Lu and Wu, 1998). From Fig. 8.2-7, there are two noticeable points: (1) with higher P_g/V level, the gas was dispersed effectively and $<K_La>$ increases sharply; (2) with the same power input, the impeller having more blades seems to give higher $<K_La>$, which implies that the appropriate increasing of the blade number will achieve an optimum design condition.

By plotting the values of $<K_La>$ vs. the product of volume average fluctuation velocity and gassing rate to the system the values of $<K_La>$ falls on a single straight line as shown in Fig. 8.2-8 regardless what is the number of blades is. This fact indicates that the product of $<u'>xQ_S$ may be closely related fluid mixing intensity for a gassed agitated vessel with a Rushton turbine impeller and can be served as a basis for scaling up .

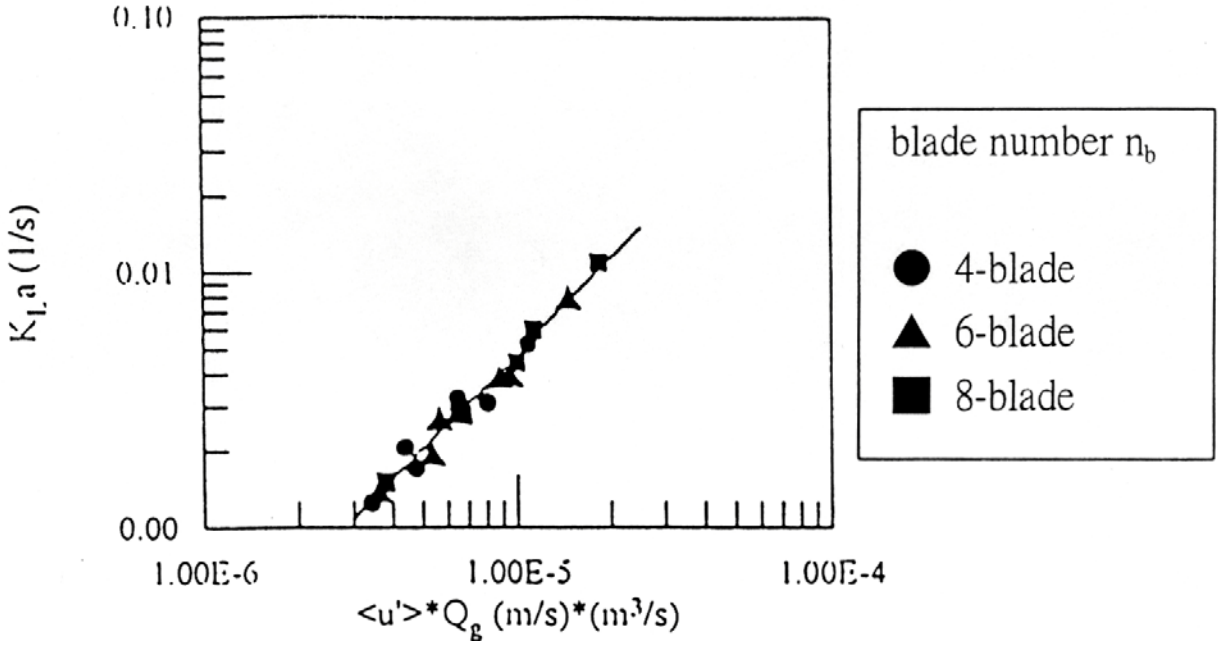

Fig. 8.2-8 Relationship between $<K_La>$and $<u'>xQ_S$ for straight blade disk turbine with various number of blad.

Correlation equations for the single Rushton turbine impeller system

To obtain a more comprehensive and useful correlation to predict the value of $< K_La>$, the mass transfer coefficient data obtained from our experiments were correlated to cover the effect of the impeller blade number, rotational speed and superficial gas velocity. The correlation was obtained as:

$$<K_La>=0.00119n_b^{0.62}N^{1.56}V_S^{0.4} \qquad (8.2\text{-}2)$$

for the single straight blade disk-type impeller agitated system and it is plotted in Fig. 8.2-9with the experimental data obtained. With this correlation the overall-averaged K_La value in the stirred vessel can be predict from a given conditions (i.e. N, Q_S and number of blades,etc.). However, in a practical scale-up practice, the power consumption per unit liquidvolume is the most popular basis adopted in the scale-up process, in order to introduce the power drawn per unit volume into this correlation, the rotational speed in Eq.(8.2-2) was replaced by the power consumption per unit volume and it can be changed as:

$$K_La=0.0297n_b^{0.1}(P_g/V)^{0.34}V_S^{0.48} \qquad (8.2\text{-}3)$$

The deviation of this correlation is less than12% and the regressive result is plotted in Fig. 8.2-10. Combining the correlations shown in Chap.6 for estimating the power drawn by the impeller and Eq.(8.2-3), one is able to estimate the required P_g/V for a gas-iquid contactor if the optimum value of $<K_La>$ is known from the laboratory scale experiment.

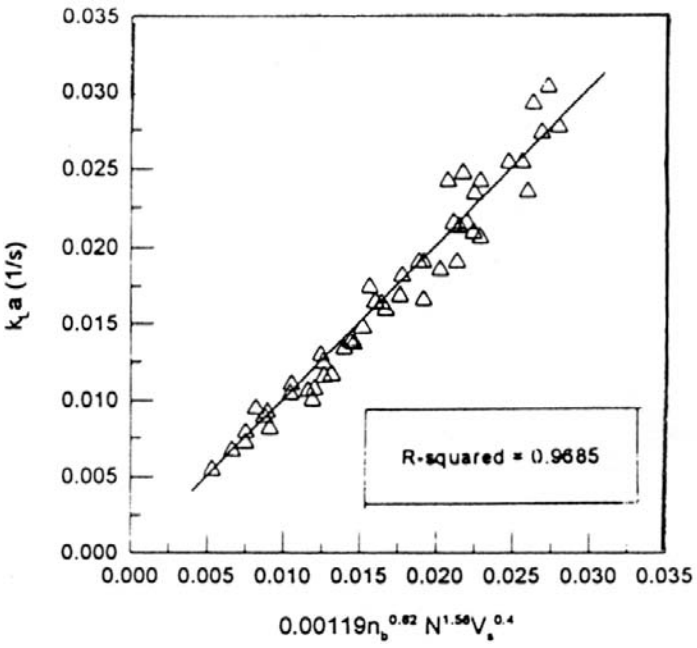

Fig. 8.2-9 Regression of $<K_La>$ for the single impeller systems based on the operating variables.

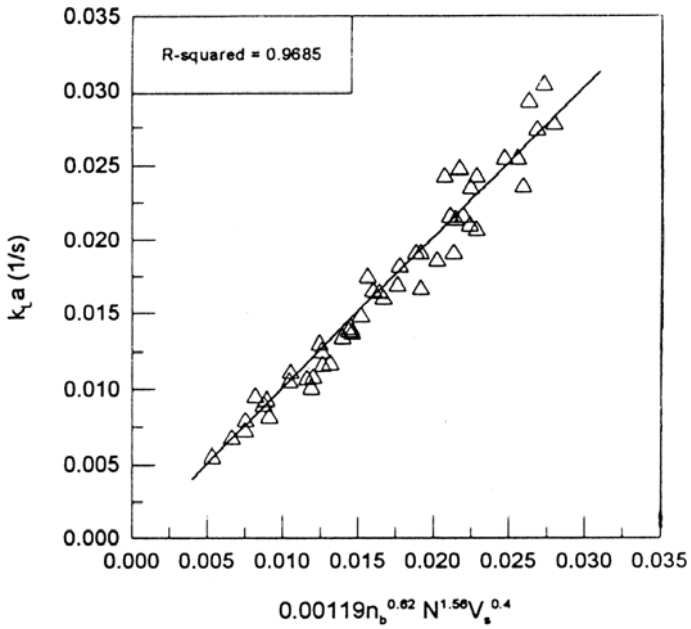

Fig. 8.2-10 <K_La> regression curve for the single impeller system based on the power consumption of impeller.

8.2.2 Comparison of mass transfer rate between Rushton turbine impeller and other type impellers

Smith turbine (Scaba turbine) impeller

The mass transfer performances of the Smith turbine impeller were examined both under a low gassing rate (Q_S=*0.5vvm*) and a high gassing rate (Q_S=*1.07vvm*) conditions and the results were compared to those of the Rushton turbine impeller with P_g/V=*557.8W/m*^{3}. Figures 8.2-11 and 8.2-12 show the local K_La distributions in the mid-plane for the cases with Q_S=*0.5vvm* and Q_S=*1.07vvm*, respectively. Based on the experimental observation, one can find that when Q_S=*0.5vvm*, both the cavity structures of these two impellers fall into the vortex cavity, under which the gas is dispersed well, and liquid pumping rate of the impeller dominates the values of local K_La. Since the power drawn by the Smith turbine impeller is always higher than that for the Rushton turbine impeller, the rotational speed of the Smith turbine impeller should be reduced to keep P_g/V the same as that for the Rushton turbine impeller. In this situation, the liquid pumping rate of the Smith turbine impeller is smaller, therefore, it gives a lower mass transfer rate than that of the Rushton turbine impeller. Increase the sparged gas rate to Q_S=*1.07vvm*, the cavity structure of the Rushton turbine impeller has changed into the large cavity, while the vortex cavity still clings to the Smith turbine impeller. Since the gas dispersion capability of the vortex cavity is much stronger than that of the large cavity, the Smith turbine impeller disperses gas more effectively and gives a higher mass transfer rate than the Rushton turbine impeller.

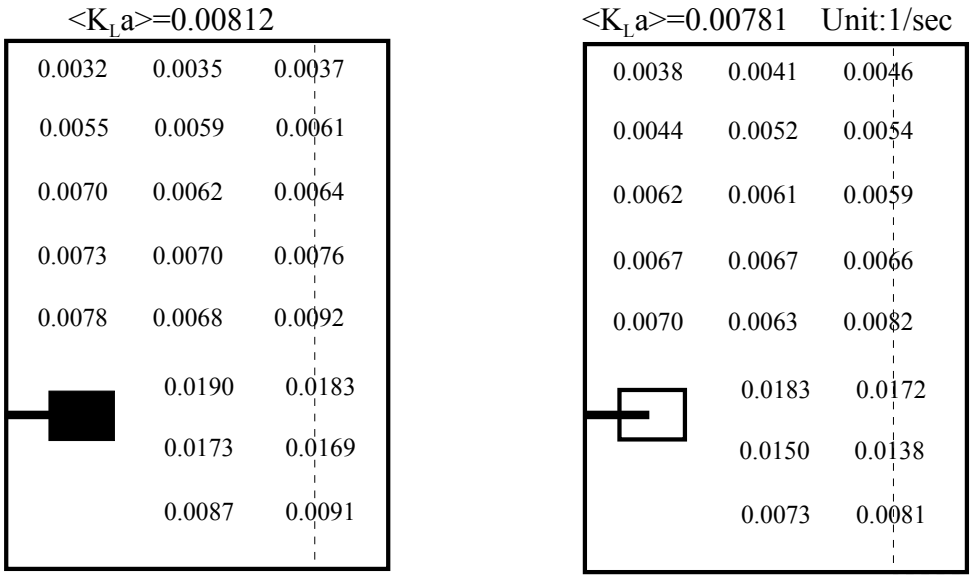

(a) Rushton turbine impeller (b) Smith turbine impeller

Fig. 8.2-11 Distributions of local K_La for the single Rushton turbine impeller and Smith turbine impeller systems with Q_S=0.5vvm and P_g/V=557.8 W/m^3.

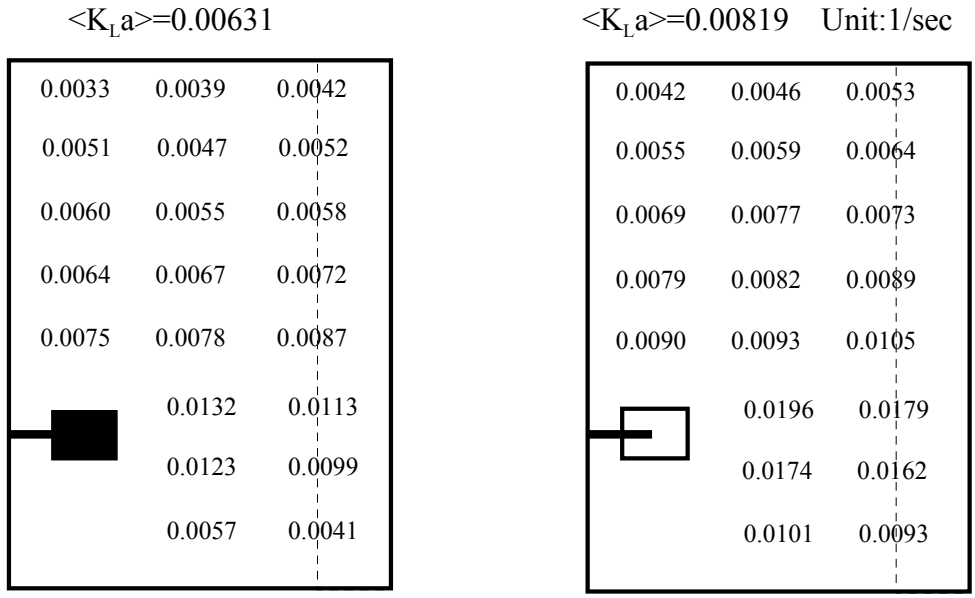

(a) Rushton turbine impeller (b) Smith turbine impeller

Fig. 8.2-12 Distributions of local K_La for the single Rushton turbine impeller and Smith turbine impeller systems with Q_S=1.07vvm and P_g/V=557.8 W/m^3.

Comparison of mass transfer characteristics of pitched paddle impeller with Rushton turbine impeller.

In Fig. 8.2-13, Distributions of liquid velocity vector and local energy dissipation rates of a mechanically agitated vessel with a single pitched paddle impeller are shown for the cases

of N=13.3rps (P/V=273.1W/m^3) and N=18.3rps (P/V=528.3W/m^3) and they are compared with the similar plot for the case of Rushton tubine impeller system. From the plots depicted in these figures, it can be seen that the larger values of energy dissipation rate always appear in the discharge stream of the impeller and decrease significantly along the circulatory loop of the liquid flow. Comparing the values of the energy dissipation rates of the pitched paddle system and the Rushton turbine systems, one can find that under the same rotational speed of N=13.3rps, the largest value of the energy dissipation rate of the Rushton turbine system is almost twice that of the value of the pitched paddle impeller system. This fact indicates that the Rushton turbine impeller can generate much high turbulent intensity and has a better gas dispersion capability than the pithed paddle impeller if the rotational sppeed of the impeller is the same. By increasing the rotational speed of the pitched paddle impeller to 18.3rps which results the power drawn by both impeller are the same, energy dissipation level of the pitched paddle impeller system will icreases to 84% of the Rushton turbine impeller system. However, under this condition, the tip velocity at paddle tip will also increase to 1.4 times of the tip velocity of Rushton turbine impeller system, which may not be preferable situation for some biological reaction systems.

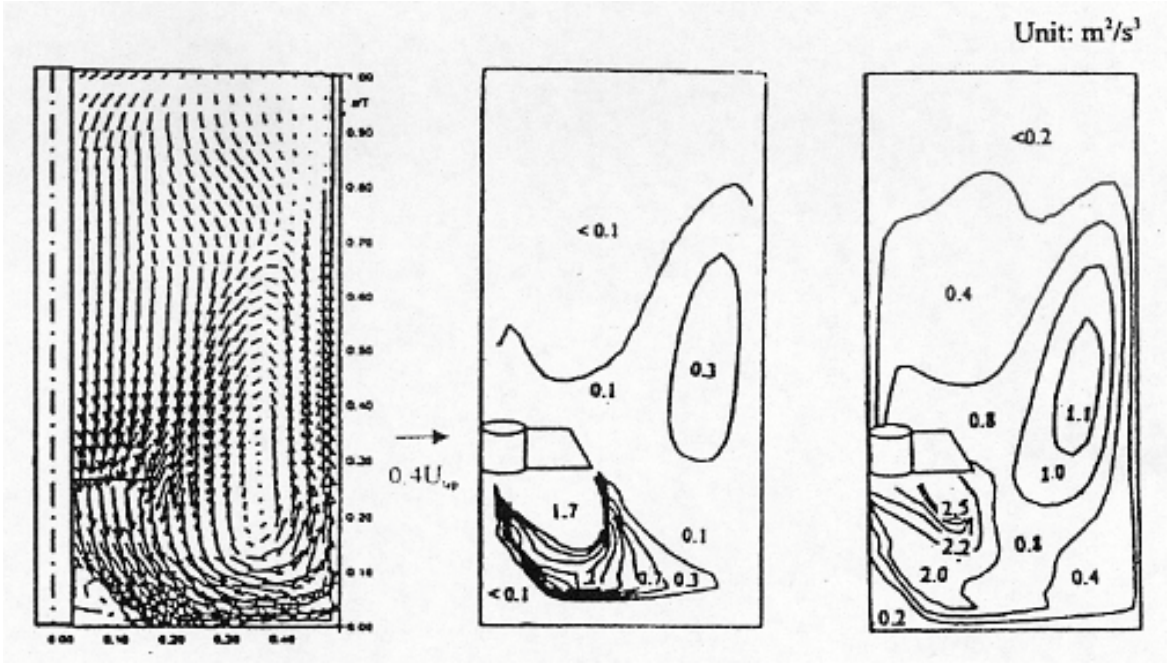

N=13.3 rps P/V=273.1 w/m^3 | N=13.3 rps P/V=273.1 w/m^3 | N=18.3 rps P/V=528.3 w/m^3

Fig.8.2-13 Distributions of velocity vector and energy disspation rates in the single pitched paddle impeller system under various rotational impeller speeds.

Although the Rushton turbine impeller generate higher energy disspation rates in the impeller discharge streams, it concentrates only in discharge region, the energy dissipation rates at the most of bulk flow region are always much lower than those for the pitched paddle impeller system. In other words, the pitched paddle impeller results in a more uniform distribution of energy dissipation rates within the agitated system. In the Table 8.2-1, comparison of tip velocity, percentage volume of dischrge region, and the ratio of average energy dissipation rate dischare in region to the average energy dissipation rate of the entire sytem are made for the systems discuused . These results show that no matter what operation condition is, more than 70% of toal energy dissipates in the discharge region of the impeller.

Table 8.2-1 Comparison of energy dispassion rate in impeller discharge regions for the Rushton turbine impeller and pitched blade impeller with Q_s=0.5 vvm and N=13.3 rps as well as P_g/V=528.3 W/m^3.

	U_{tip}(m/sec)	V_D/V_T(%)	$\varepsilon_D/\varepsilon_T$(%)
Rushton turbine impeller (N=13.3 rps, P_g/V=528.3 W/m^3)	1.968	9.0	85.0
Pitched blade impeller (N=13.3 rps, P_g/V=273.1 W/m^3)	1.968	14.1	70.0
Pitched blade impeller (N=18.3 rps, P_g/V=528.3 W/m^3)	2.707	14.1	68.7

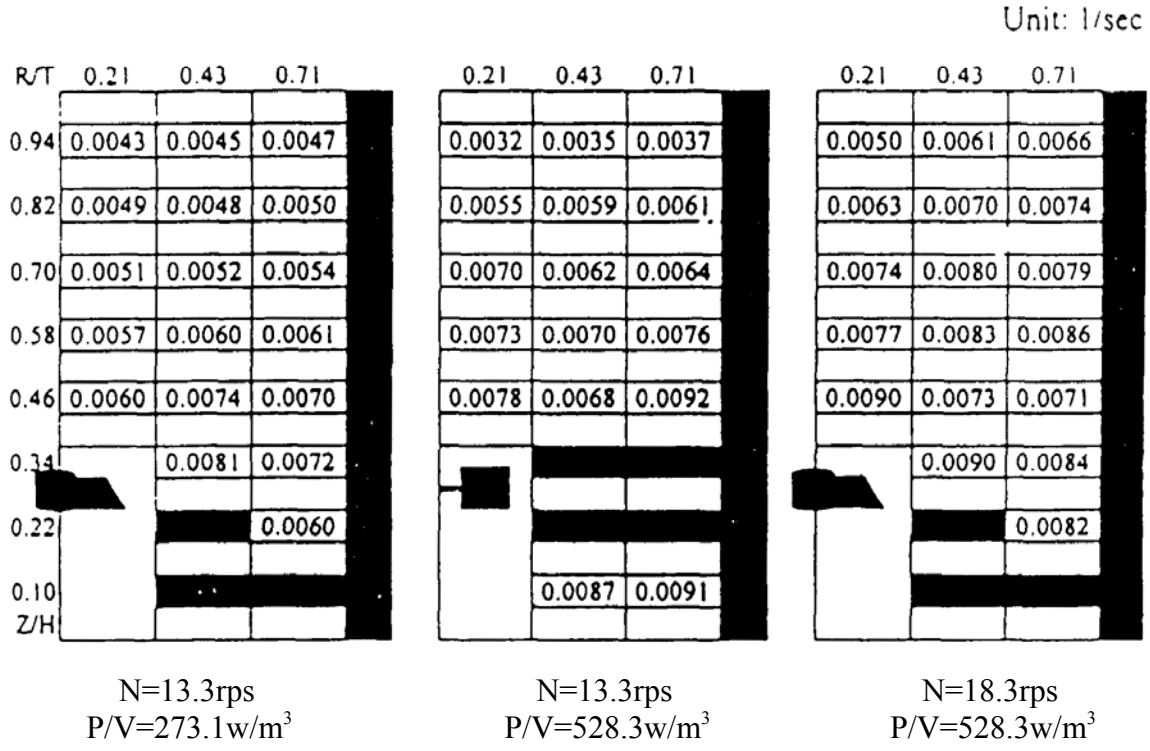

N=13.3rps P/V=273.1w/m^3 | N=13.3rps P/V=528.3w/m^3 | N=18.3rps P/V=528.3w/m^3

Fig. 8.2-14 Distribution of local mass transfer coefficients in vraious single impeller systems.

To examine how the energy dissipation rate relates to the mass transfer rate, the local mass transfer coeficient in single Rushton turbine and single pitched paddle impeller systems were determined by using the N_2 gassing out method. Fig. 8.2-14 depicts the results of the measurements. It is found that nonuniform distribution of K_La exists for both systems and the highest mass transfer rate always appears in the discharge stram of the impeller and decays quickly along the circulatory loop. This trend is quite similar to the trends observed in the cases of energy dissipation rate distributions. Table 8.2-2 lists a comparison of average mass transfer coefficients for the pitched paddle impeller system under different impeller rotational speeds with the same distribution for the Rushton turbine system. Under the same rotional speed, the Rushton impeller system exhibits 1.5 times larger mass transfer rate,which elucidates the importance of high gas dispersion capability of the Rushton impeller.With the same power input, the pitched paddle system gives almost the mass transfer rate as the Rushton turbine system. Since the pitched paddle can produce larger pumping and circulating rates under the same rotational speed, therefore, a combination of Rushton turbine impeller with pitched paddle impeller can be a good design for providing a more homogeneous mass transfer rate and solute concentration distributions for lager volume systems.

Table 8.2-2 Comparison of mass transfer rates between pitched paddle and Rushton turbine impeller systems.

	$<K_La>$(1/s)	$<K_La>_D/<K_La>$(%)	V_D/V_T(%)
Rushton turbine impeller (N=13.3 rps, P_g/V=528.3 W/m^3)	0.00812	30.1	9.0
Pitched blade impeller (N=13.3 rps, P_g/V=273.1 W/m^3)	0.00627	20.3	14.1
Pitched blade impeller (N=18.3 rps, P_g/V=528.3 W/m^3)	0.00807	23.2	14.1

8.2.3 Effect of Gassing rate on mass transfer rate in single impeller systems

Table 8.2-3 lists the power drawn and the overall average mass transfer coefficients for the Rushton turbine impeller and pitched paddle impeller systems with N=13.3rps under different gassing rate conditions. The data in this table show that under a given rotational speed the pitched blade impeller with the same diameter draws less power than the Rushton turbine impeller no matter what the value of the gassing rate is. Since the Rushton turbine impeller has better gas dispersion capability, it disperses gas more completely and can recirculate bubbles back into the impeller region even under a higher gassing rate condition, which further reduces the power drawn by the impeller. Therefore, the difference in the values of the ratio of power drawn by the pitched blade impeller and to the Rushton turbine impeller

becomes smaller under a higher aeration condition. As gassing rate is smaller than 0.5vvm, gas is dispersed completely and the circulating flow of liquid dominates the mass transfer rates. Under this circumstance, the pitched paddle impeller can reach more than 80% $<K_La>$ of the Rushton turbine impeller, while it draws only about 50% of the power of the Rushton turbine impeller. However, once the gassing rate exceeds 0.8vvm, the pitched blade impeller can not disperse the sparged gas effectively and the gas dispersion capability of the impeller dominates the mass transfer rate, under which the Rushton turbine impeller produces more than 50% higher $<K_La>$ than that of the pitched paddle impeller.

Table 8.2-3 The overall average mass transfer coefficient and the ratio of power drawn for the Pitched paddle impeller to Rushton turbine impeller and pitched blade impeller under various aeration rates with N=13.3rps.

$<K_La>$(1/s) / Q_S (L/min)	$<K_La>_R$	$<K_La>_P$	$P_{g(P)}/P_{g(R)}$	$<K_La>_P/<K_La>_R$
0.5(0.22vvm)	0.00732	0.00623	0.494	0.851
1.0(0.44vvm)	0.00872	0.00711	0.516	0.804
2.0(0.88vvm)	0.0153	0.00713	0.608	0.466
3.0(1.32vvm)	0.0184	0.00726	0.682	0.395
4.0(1.76vvm)	0.0211	0.00738	0.773	0.350
5.0(2.20vvm)	0.0213	0.00726	0.776	0.341
6.0(2.64vvm)	0.0215	0.00725	0.781	0.337

In Fig. 8.2-15, the traditional plots of $<K_La>$ vs. the gassing rate, Q_S as well as the superficial velocity V_S for these two different systems under various rotational speeds are shown. In these plots, the value of $<K_La>$ increases with the increase in the gassing rate under a lower aeration condition, and a leveling-off value of $<K_La>$ is exhibited in these curves as the gassing rate exceeds a certain value for a given rotational speed. It is interesting to note that the pitched paddle impeller may perform as well as the Rushton turbine impeller if the gassing rate is smaller than 0.5vvm, but it soon reaches a leveling-off value as the gassing rate exceeds certain limit (Q_S>0.5vvm). However, the $<K_La>$ value given by the Rushton turbine impeller shows a sharp increase due to the increase in the rotational speed and can continuously increase to the higher gassing rate due to its superior gas dispersion capability.

From results shown in above, it can be seen that the mass transfer rate within the stirred vessel is severely controlled by the motion of bubbles within the stirred vessel. Although the bubble motion enhances the liquid mixing, the bubbles coalesce intensively under this

situation, making the mass transfer rate mostly independent of the gassing rate.

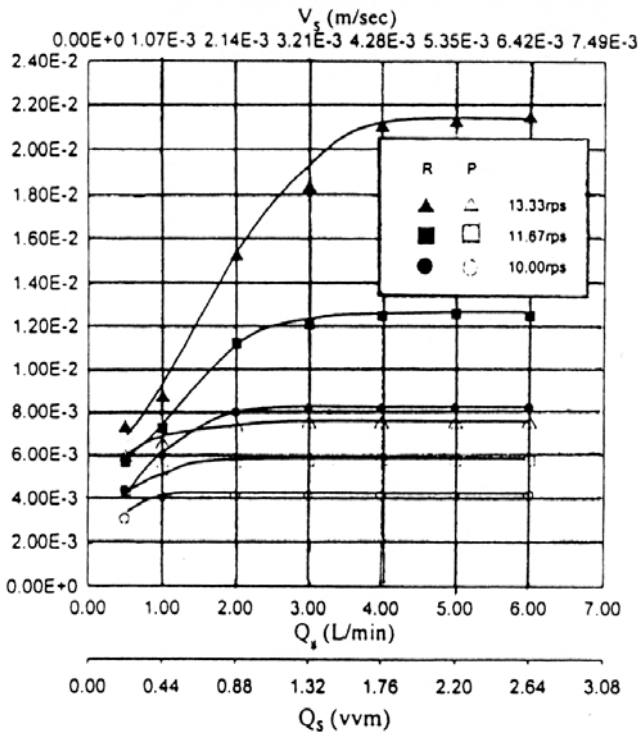

Fig. 8.2-15 Effect of the gassing rate on the overall average mass transfer coefficient for the single impeller systems under various rotational speeds.

8.3 The Role of the gas recirculation rate on the mass transfer

To illustrate the role of gas recirculation in the mass transfer process, the local mass transfer coefficients were determined in the two different size gassed agitated vessels, equipped with the same size Rushton turbine impeller, which will give the D/T ratio as 1/3 and 1/6. Fig.8.3-1 depicts the flow patterns of bubbles within these two different diameter vessels. Under the condition N=13.3 rps and gassing rate =0.5vvm, no obvious gas recirculation back into impeller region can be seen in the larger vessel, while substantial bubbles are recirculated into the impeller region in the small vessel system. The results of the local mass transfer coefficients for both systems are depicted in Fig.8.3-2. Since the bubbles did not recirculated back into the impeller region in the large vessel system, the power drawn by impeller for this system is 28% higher than that of the small vessel system. These data are summarized in Table 8.3-1, which also shows that the system without gas recirculation results in 20% lower mass transfer rate in discharge region of impeller and 50% lower in volume average mass transfer rate confined within the imaginary bounded volume of the larger vessel as it is compared with the small vessel system. This fact indicates that negligence of gas recirculation in the study of the transport properties in a gassed mechanically agitated vessel may cause erroneous conclusion.

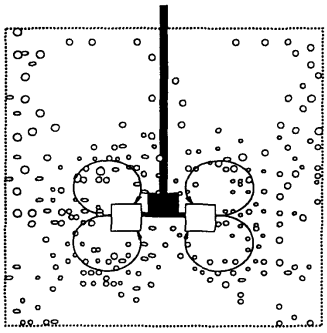

(a) D/T=1/3, with gas recirculation

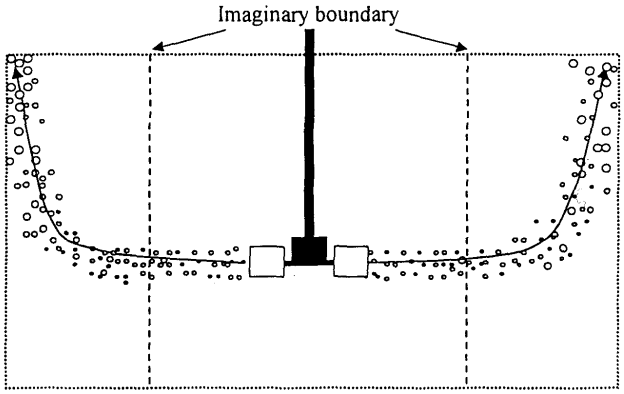

(b) D/T=1/6, without gas recirculation

Fig.8.3-1 Flow patterns of bubbles in two different diameter vessels.

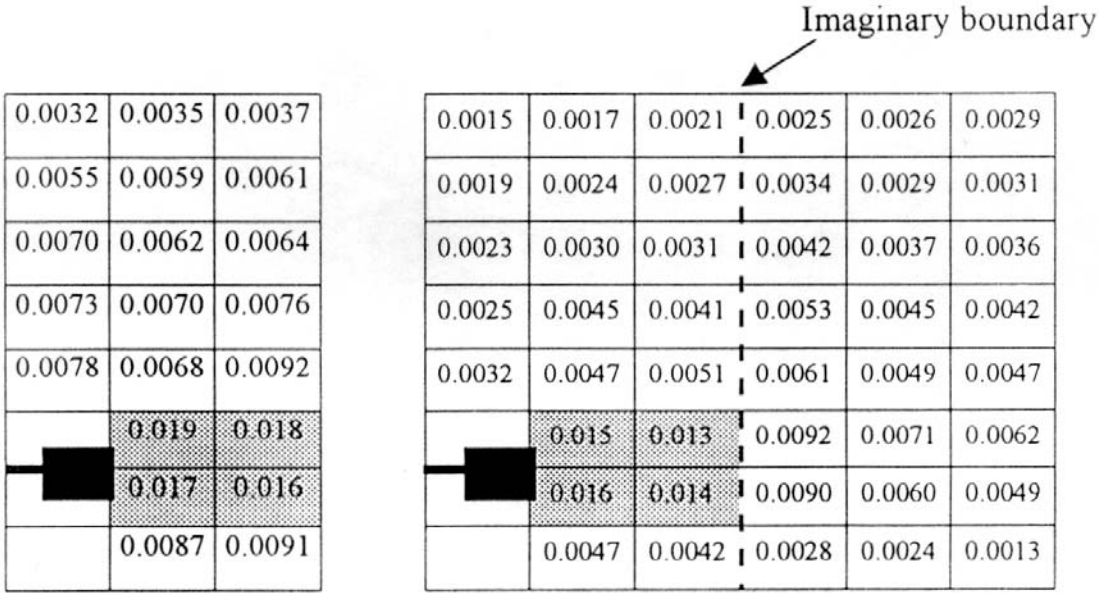

(a) N= 13.3 rps, P_g/V=528.3 W/m^3 T=0.141 m, D/T=1/3

(b) N= 13.3 rps, P_g/V=676.2 W/m^3 T=0.288 m, D/T=1/6

Fig. 8.3-2 Distributions of local mass transfer coefficient in two different diameter vessels, under conditions of N=13.3rps and Q_S=0.5vvm.

Table 8.3-1 Comparison of mass transfer rates in impeller discharge stream and average mass transfer rate in two different diameter vessels.

Impeller System	(I) T=0.141m,D/T=1/3	(II) T=0.288m,D/T=1/6	(II)/(I)×100%
$<K_La>_D$	0.018	0.015	74.5
$<K_La>$	0.0082	0.0043	49.8

Without considering the effect of gas recirculation, Bakker (1992) used a CFD method to evaluate the local mass transfer coefficient in systems equipped with a single Rushton turbine impeller, an A315 impeller or a pitched blade impeller. He showed that approximately 30% of the overall mass transfer occurred within 7.8% of the liquid volume just around the Rushton turbine impeller, while only 14% and 12% of the overall mass transfer took place in the impeller regions for the A315 impeller and pitched impeller systems, respectively.

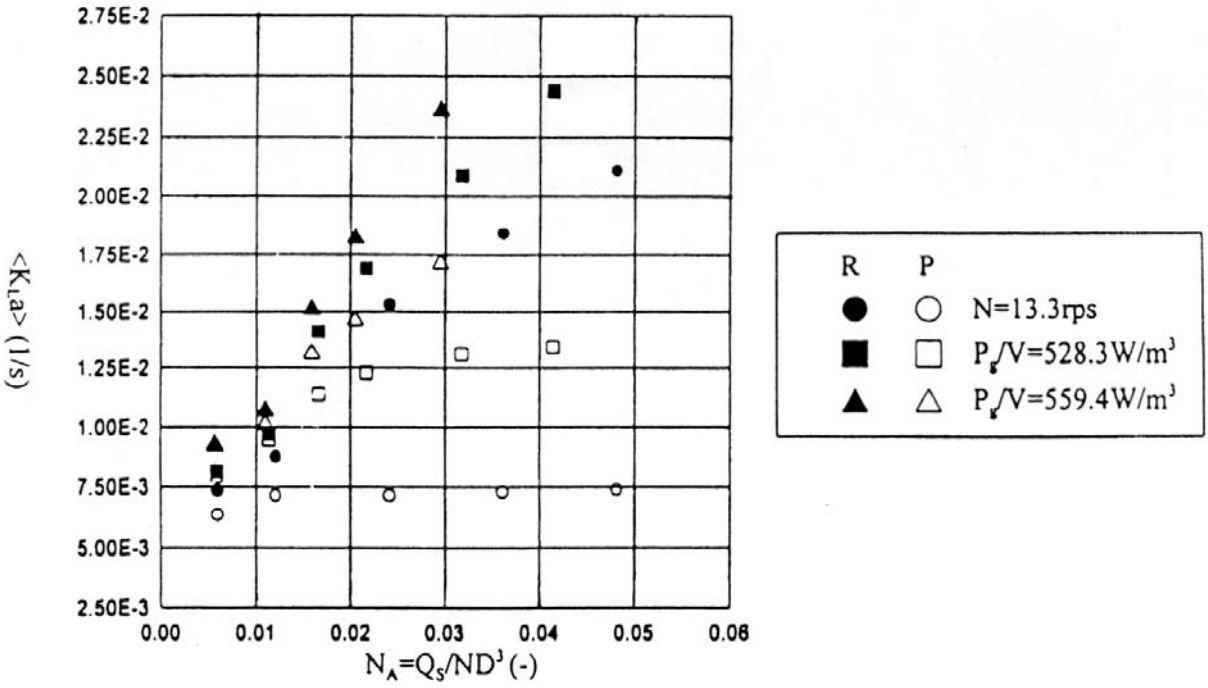

Fig. 8.3-3 The traditional plot of $<K_L>$ vs. gas flow number($=Q_S/ND^3$).

Since both the recirculated gas as well as the sparged gas passes through the impeller region, these two gas streams contribute to the reduction of the power drawn by the impeller and severely affect gas dispersion within the stirred vessels. Recently, Takenaka and Takahashi (1996) integrated the local gas holdup in the regions beneath the impeller to estimate the gas recirculation rate for a Rushton turbine impeller system. They concluded that the correlation based on total gassing rate is more appropriate than that based on the sparging gas rate for the overall gas holdup estimation. However, in their study the recirculated bubbles

from the regions above the impeller were neglected, which perhaps causes an underestimation of the actual gas recirculation rate. Many correlations have been proposed in the literature to estimate the value of $<K_La>$, while the overall mass transfer coefficient has always been correlated with the sparged gas rate or the superficial gas velocity only, which neglects the effect of the recirculated gas. The results obtained in our studies indicated that the amount of recirculated gas could be four times the amount of gas originally sparged into the impeller through the gas spager. Since both power drawn by the impeller and the rate of mass transfer around the impeller is closely related to the amount of gas bubbles around the impeller, prior to grasp the exact situation of transport processes occurred around the impeller, it is necessary to have the net gassing rate to replace the gassing rate originally fed through the gas sparger. The net or total gassing rate can be estimate by summing up the original gassing rate and gas recirculating rate around the impeller. Fig. 8.3-3 shows the plots of $<K_La>$ vs. the traditionally defined gas flow number ($=Q_S/ND^3$) for the Rushton turbine impeller and the pitched paddle impeller. From the data points shown in this figure, one can find that all the data points spread in a quite scattered matter. However, using the net or total gassing rate, Q_t, to replace the originally gassing rate through the sparger, Q_S, the relationship between $<K_La>$ and the **modified aeration number $N_A'(=Q_t/ND^3)$** for different impellers can be regressed on a single straight line as shown in Fig. 8.3-4. From this result, it is found that no matter what the rotational speed is, the values of $<K_La>$ always increases with the increase in N_A' when the gas dispersion regime within the vessel is beyond stage(c). Therefore, it can be concluded that the total gassing rate is more appropriate and reasonable than the sparging gas rate for correlating the $<K_La>$ value in a gassed mechanical agitated vessel. These data can be correlated as:

$$<K_La> = 0.134\ (Q_t/ND^3) + 0.00339 \qquad (8.3\text{-}1)$$

for both the single Rushton turbine impeller and the pitched blade impeller systems and deviation is less than 15% with Eq.(8.3-1). To examine the applicability of Eq.(8.3-1), the measured $<K_La>$ values for the Smith turbine impeller along with those for the Rushton turbine impeller are plotted with this correlation and the results are shown in Fig.8.3-5. Where the total gassing rate around the impeller was acquired through the approach proposed by Lu et al. (1999). From the data points shown in this figure, it can be seen that regardless of the aeration rate, once the gas is dispersed well, this correlation can not only be used to predict the mass transfer rate of the Rushton turbine impeller, but also the Smith turbine impeller.

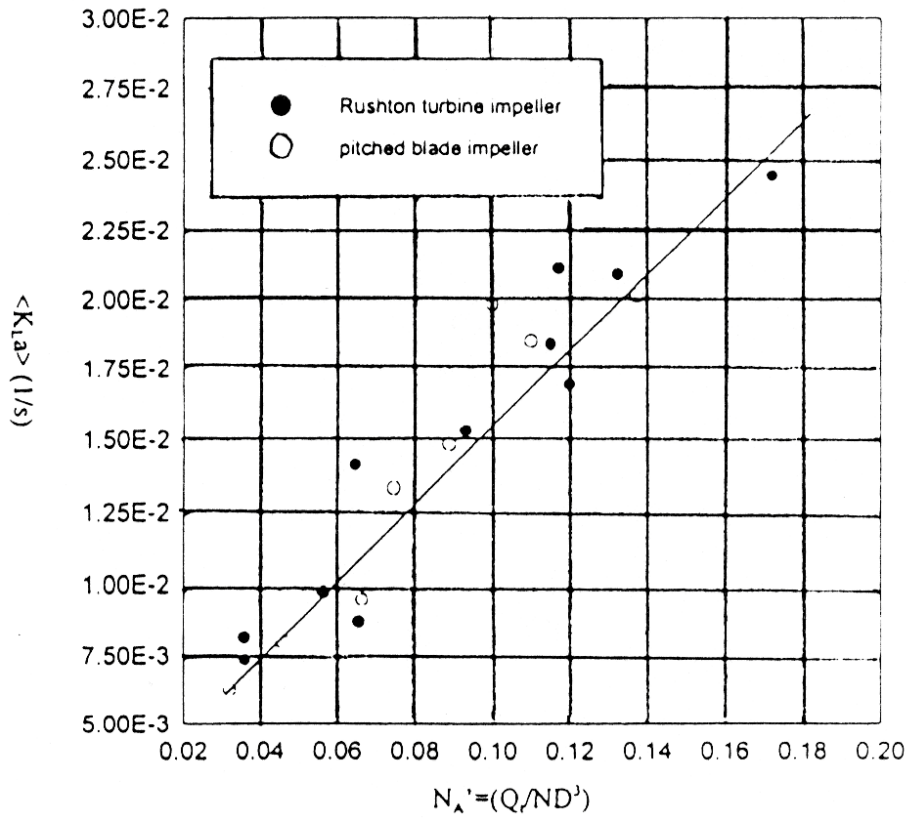

Fig. 8.3-4 The correlation of $<K_La>$ against the net gassing rate Q_t.

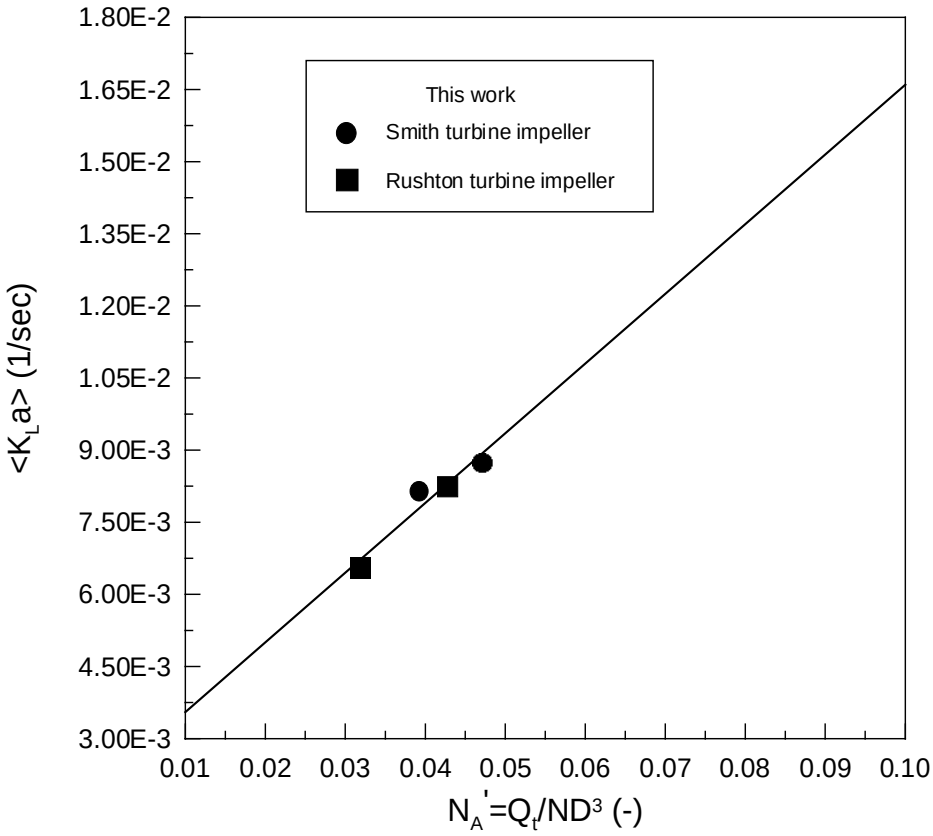

Fig. 8.3-5 Application of Eq. (8.3-1) to Smith turbine impeller.

8.4 Mass Transfer Charateristics in Multiple Impellers Systems

As it was mentioned, high aspect ratio gas-liquid contactors with a multiple impeller design have been employed in order to have larger interfacial area between gas and liquid phases and more uniform distribution of shear level within a gassed mechanically agitated vessel. In designing such a system, the detail knowledge of the mass transfer coefficients within the system becomes indispensable.

In a multiple impeller system, the non-uniform gas loading and different power drawn among each impeller have attracted many attentions (Nienow and Lilly, 1979; Smith et al., 1987; Nocentini, 1988; Linek et al., 1996; Mochizuki, 1992; Lu and Yao, 1992; Lu and Chiu, 1995; Cui et al., 1996). Since both of them play important roles in the mass transfer around each impeller, they should be kept in mind during discussing the performance of g-l mass transfer in a gassed agitated vessel with multiple impellers. Without considering the non-uniform power drawn and effect of gas recirculation around each impeller, Nocentini et al. (1993) studied the mass transfer rate in systems equipped with triple or quadruple Rushton turbine impellers and presented

$$<K_La>=0.015(P_g/V)^{0.59}V_S^{0.55} \tag{8.4-1}$$

to predict the averaged mass transfer rate within the air-water system. By imposing the exponent of gas superficial velocity as 0.4, Nocentini et al. (1993) proposed another correlation with slight accuracy reduction as:

$$<K_La>=0.0055(P_g/V)^{0.62}V_S^{0.4}, \tag{8.4-2}$$

Eq.(8.4-2) was very similar to the correlation

$$<K_La>=0.00495(P_g/V)^{0.59}V_S^{0.4} \tag{8.4-3}$$

proposed by Linek et al. in 1987for a single Rushton turbine impeller system. Whence, they concluded that no matter for single or multiple impeller systems; energy dissipation density and gas superficial velocity were sufficient to determine the mass transfer performances of agitated vessels.

Moucha et al. (1995) used “dynamic pressure-step method” to determine the mass transfer coefficient for each impeller region in the four Rushton turbine impeller systems. They pointed out that since the amount of gas passing through upper impellers is much less than that for the bottom impeller, it results in a higher power dissipation but lower mass transfer rate in upper impeller regions. The same method was also adopted by Linek et al. (1996) to measure the mass transfer coefficient for each impeller stage in the system the same as the one used by Moucha et al.(1995). They proposed different correlation equations to predict the mass transfer rate for the bottom and upper impellers, respectively and the effect

of the liquid property (i.e. coalescing or coalescing) was also taken into account.

Considering the recirculated gas both from the regions above and below impeller, the authors (Lu et al., 2000) evaluated the average mass transfer coefficients for different impeller in single impeller systems and presented a straight line in the plot of $\langle K_L a \rangle_D$ vs. (Q_t/ND^3) for single impeller systems, which could be expressed as:

$$\langle K_L a \rangle_D = 0.134\ (Q_t/ND^3) + 0.00339 \qquad (8.4\text{-}4)$$

In this section, mass transfer characteristic of multiple impeller system is discussed by recapitulating the phenomenon of gas recirculation around each impeller and a generalized correlation for estimating $\langle K_L a \rangle$ around each impeller region in multiple impeller system will be presented.

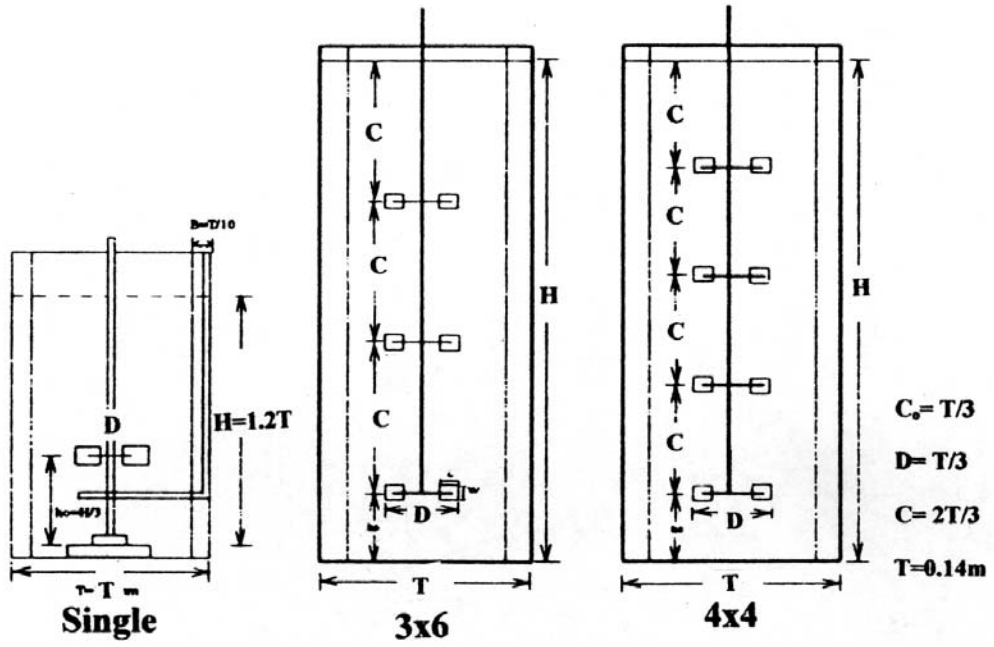

Fig.8.4-1 The sketch of the Two different multiple impellers vessels.

8.4.1 Multiple Rushton Tubine impellers systems

From the results shown in Fig.8.2-3, it is interesting to compare the overall performances of gas dispersion in the two multiple impeller systems as shown in Fig. 8.4-1 equipped with triple stages of 6-blade impellers(3×6) (standard Rushton turbine impellers) and a system equipped with quadruple stages of 4- straight blades impellers(4×4). Table 8.4-1gives a comparison of average mass transfer rates of these two different multiple impeller vessels under gassing rate of Q_S=0.22vvm and N=13.3 rps while Tble 8.4-2 shows the same comparison except Q_S=0.757vvm. In a lower gassing rate, it is surprising to note that the 4×4 system gave 14% higher $\langle K_L a \rangle$, while it drew 17.5% less total power consuption than the 3×6 system. However, this trend will reverse as the gassing rate exceeds 0.757vvm as given in Table 8.4-2. Under a high gasing rate, the 4×4 system drew less than 26.7% power, and gave

less than 18.3% on average of K_La value. If the power for the 4×4 system was increased to the same level as the 3×6 system at the same gassing rate, the average values of K_La for both svstems are nearly the same, as shown in Table 8.4-3.

Table 8.4-1 Comparison of the <K_La> values between 4×4 and3×6 impeller systems under a very low gassing rate (Q_S=1.2L/min=0.22vvm) and N=13.3rps.

	$<K_La>$	$<K_La>$ Ratio	Power Ratio
3×6 (Ⅰ)	0.0211	1	1
4×4 (Ⅱ)	0.0241	1.142	0.825
(Ⅱ - Ⅰ)/ Ⅰ %	+14.2 %	+14.2 %	-17.5 %

Table 8.4-2 Comparison of the <K_La> values between 4×4 and3×6 impeller systems under a high gassing rate (Q_S=3.97L/min=0.757vvm) and N=13.3rps.

	$<K_La>$	$<K_La>$ Ratio	Power Ratio
3×6 (Ⅰ)	0.0313	1	1
4×4 (Ⅱ)	0.0256	0.817	0.733
(Ⅱ - Ⅰ)/ Ⅰ %	-18.3 %	-18.3%	-26.7 %

Table 8.4-3 Comparison of the <K_La> values between 4×4 and3×6 impeller systems under a high gassing rate (Q_S=3.97L/min=0.757vvm) and P_g/V=1004.4W/m^3.

	3×6 impeller system	4×4 impeller system
$<K_La>$	0.0313	0.0308
Ratio of $<K_La>$	1	0.982
Ratio of power consumption	1	1

These differences wre due to flooding occurred at the lowest impeller in 4×4 qurdaple impeller under gassing rate of Q_S=0.757vvm, therefore, this system gave a lower average mass transfer rate than the system with 3 standard Rushton impellers. However, if the flooded region was excluded from the counting of the average value of K_La, the remaining part of the 4×4 system still performed as well as the 3×6 system, as shown in Table 8.4-4 This fact implies that the increase in the number of blades may have a better gas handling capability of the impeller, but too many blades (or too narrow blade pitch) will disturb the formation of a strong vortex, which again will weaken the capability of gas dispersion as shown in Fig.8.2-3.

Table 8.4-4 ffect of the flooding phenomenon of the lowest impeller of the 4×4 and3×6 impeller system on <K_La> under a higher aerated rate (Q_S=3.97L/min=0.757 vvm) and N=13.3rps.

	3×6 (Ⅰ)	4×4 (Ⅱ) lowest impeller included	4×4 (Ⅲ) lowest impeller included
$<K_La>$	0.0313	0.0308	0.0318
$<K_La>$ ratio	1	0.98	1.016

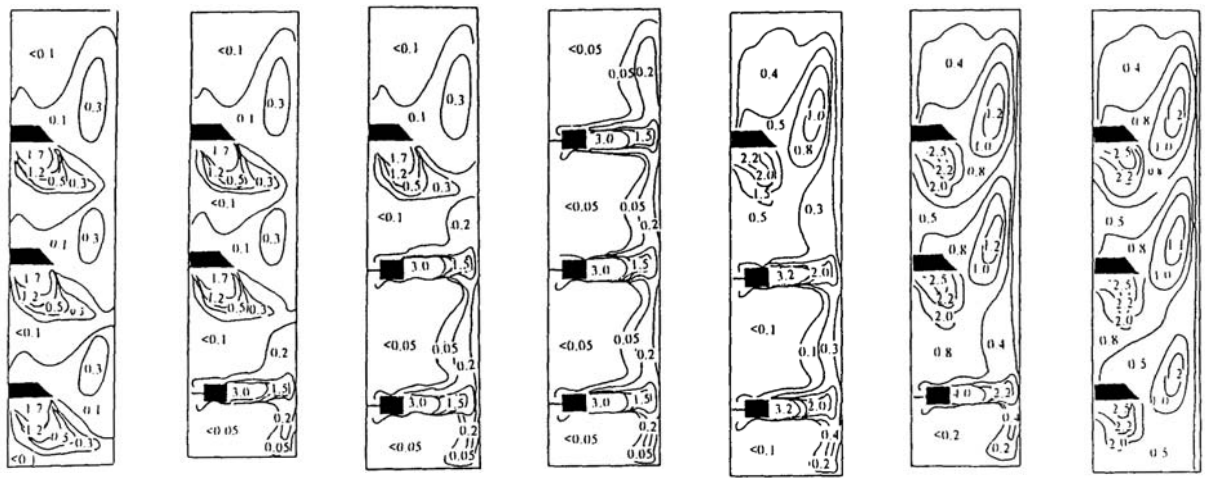

(a) N=13.3 rps (b) N=13.3 rps (c) N=13.3 rps (d) N= 13.3 rps (e) N= 14.7 rps (f) N= 16.0 rps (g) N=18.7 rps

(a) P_g/V=580W/m^3 (b) P_g/V=700W/m^3 (c) P_g/V=851W/m^3 (d) P_g/V=1004W/m^3 (e) P_g/V=1004W/m^3 (f) P_g/V=1004W/m^3 (g)P_g/V=1004W/m^3

Fig. 8.4-2 Contours of the calculated energy dissipation rate (ε) for various multiple impeller systems in the mid-plane (45^o) under *N=13.3rps* as well as P_g/V=1004.4W/m^3.

8.4.2 Multiple Impeller system with various impeller combinations

Energy dissipation rate for systems equipped with various impeller combinations

Figure 8.4-2 depicts the contour plots of the calculated energy dissipation rate ε in mid-plane (45^o) for the RRR, PRR, PPR and PPP impeller systems without gassing, under constant rotational speed N=13.3rps or the same power input P_g/V=1004.4W/m^3. It is found that larger ε values always appear in the impeller discharge stream and decay significantly along the liquid circulating loop. For the RRR and PPP systems, contours of energy dissipation rate around each impeller are very similar, which implies that if the clearance between impellers is large as 2D, each impeller can be deemed as independent. With the same rotational speed, the largest ε value for the Rushton turbine impeller is almost twice of the largest ε found in the discharge stream of the pitched paddle impeller. This fact indicates that the Rushton turbine impeller provides a higher turbulent intensity and possesses a better gas dispersion than the pitched paddle impeller. Because of the less power drawn by the pitched paddle impeller under the same rotational speed, to have the same values of P_g/V, the systems with at least a pitched paddle impeller, such as the PRR, PPR and PPP systems should be operated with higher rotational speeds than the RRR system. Under this condition, they exert stronger pumping rates due to the increase in the rotational speed of each impeller. Furthermore, the lowest Rushton turbine impeller in the PRR and PPR systems also dissipates more energy than that in the referential RRR system and may result in a higher turbulent intensity and a better gas dispersion. However, even with the same energy dissipation density, the largest ε

value around each impeller in the PPP system is still much smaller than those around the Rushton turbine impellers in other systems. This fact indicates that as long as gas is not well dispersed, it is impossible to have a higher value of $<K_La>$, even with a stronger liquid circulation or a more uniform distribution of energy dissipation rate as seen in the PPP system.

8.4.3 Distributions of Local Mass Transfer Coefficients in multiple impeller systems

Figure 8.4-3 shows the comparison of the experimentally determined local K_La in three different azimuthal planes for the RRR system with T=0.141m, Q_{S1}=0.5vvm and N=13.3rps. From the data shown in this figure, one can find that the largest mass transfer rate always appears in the impeller discharged stream, where the dispersed bubbles are smaller, gas holdup values are higher and the turbulent intensities are larger. Departing from the discharge region of impeller, the turbulent intensity decays and dispersed bubbles coalesce, which results in a lower mass transfer rate. Comparing the distributions of K_La in different azimuthal planes, no obvious difference in K_La was observed except at the locations behind the baffle plate, where K_La values are much larger. Both the calculated flow patterns from this study and the experimental results obtained by Lu and Chiu (1995) showed that there is a stronger upward flow along tank wall behind the baffle plate, which collects more dispersed bubbles and may give higher mass transfer rates along vessel wall.

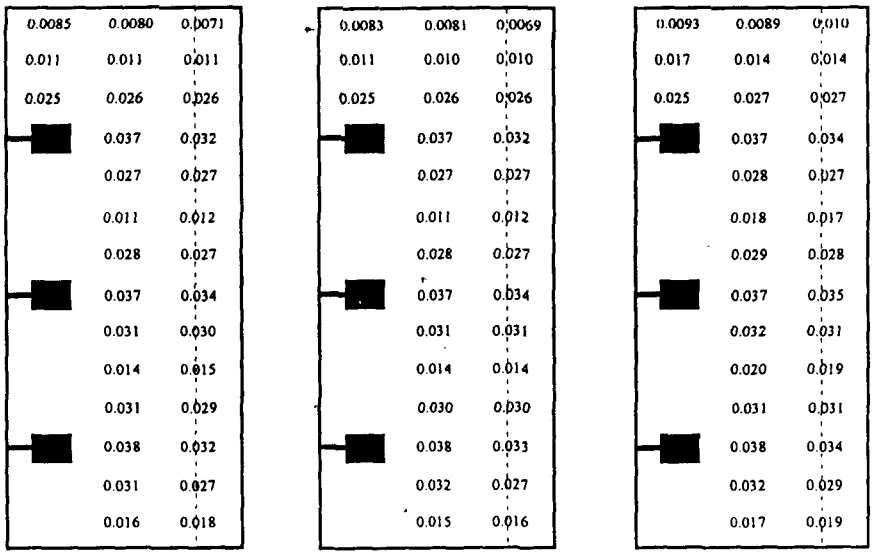

(a) in front of baffle(+10°) (b) mid-plane(45°) (c) behind baffle(-10°)

Fig. 8.4-3 Distributions of local K_La value in three different azimuthal planes systems for *RRR* system with *N=13.3rps, T=0.141m* and Q_S=*0.5vvm*.

Similar plots of local mass transfer coefficient distributions were for the systems having various impeller combinations with a given gassing rate of Q_{S1}=0.5vvm(=2.57L/min) under

the same rotational speed condition of N=13.3rps along with the identical energy dissipation density $P_g/V=1004.4.W/m^3$ were given in Fig. 8.4-4. Comparing the K_La distributions shown in these figures to the contour plots of energy dissipation rates given in Fig.8.4-2, it is found that all the trends of the variation in K_La values in these figures are very similar to the distribution of ε shown in Fig.8.4-2. The highest mass transfer rate always appears in the discharge region of the impeller, where the turbulent intensity is the highest and dispersed bubbles are smaller. Along with the circulating loop, gas bubbles coalesce and the energy dissipation rate decrease, which makes the decrease in K_La along the liquid circulating loop. With the enforcement of the axial flow from the upper-pitched blade impeller, the Rushton turbine impeller beneath the pitched blade impeller always provides a stronger fluid circulating flow. It circulates more dispersed bubbles back into the impeller region; hence gives a much higher gas holdup level and larger K_La values around the impeller. Since the Rushton turbine impeller performs a better gas dispersion, the mass transfer rates around the Rushton turbine impeller in each system are always 1.5 times higher than that around the pitched blade impeller. However, once departing from the impeller region, the circulating flow rate provided by the pitched blade impeller will dominate mass transfer rate and gives higher K_La in bulk region of the stirred vessel, and also result in a higher $<K_La>$.

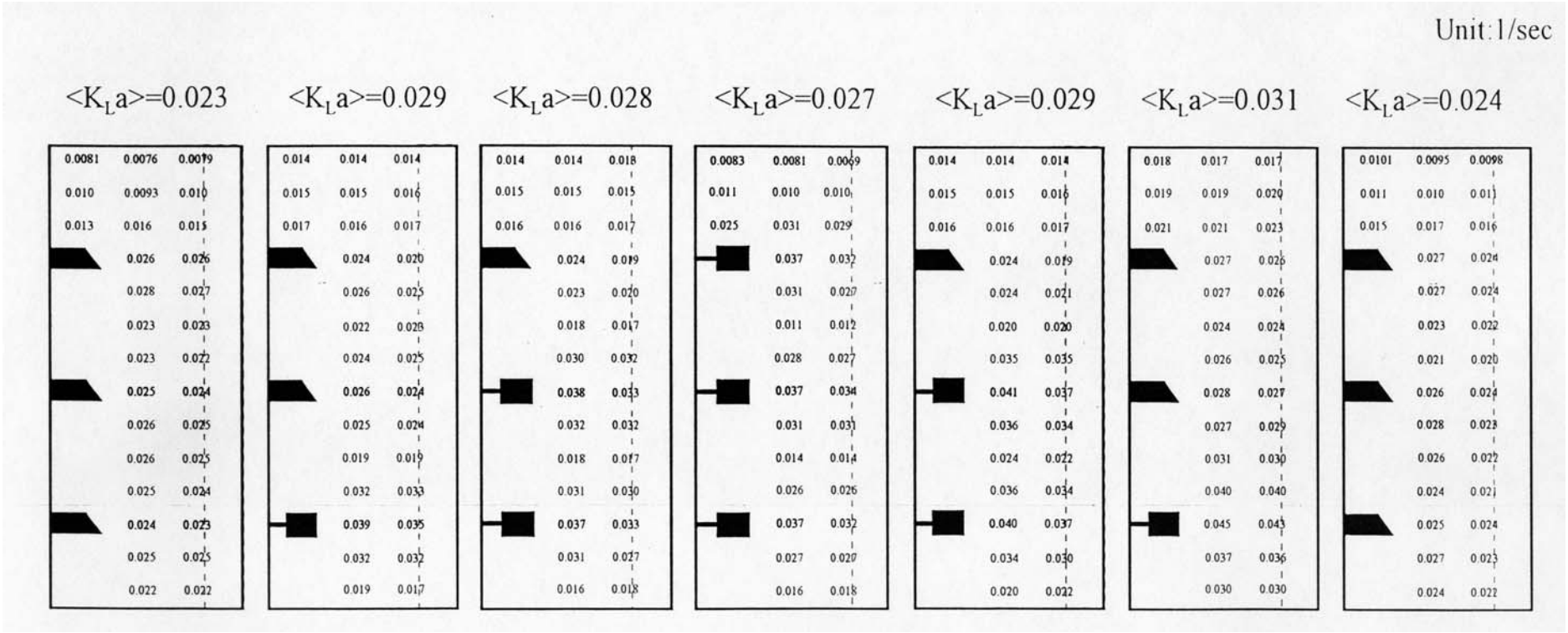

(a) N=13.3rps P_g/V=580W/m^3 (b) N=13.3rps P_g/V=700W/m^3 (c) N=13.3rps P_g/V=851W/m^3 (d) N=13.3rps P_g/V=1004W/m^3 (e) N=14.7rps P_g/V=1004W/m^3 (f) N=16.0rps P_g/V=1004W/m^3 (g) N=18.7rps P_g/V=1004W/m^3

Fig. 8.4-4 Distributions of the local K_La value for various multiple impeller systems in the mid-plane (45^o) with *N=13.3rps* and P_g/V=1004 W/m^3.

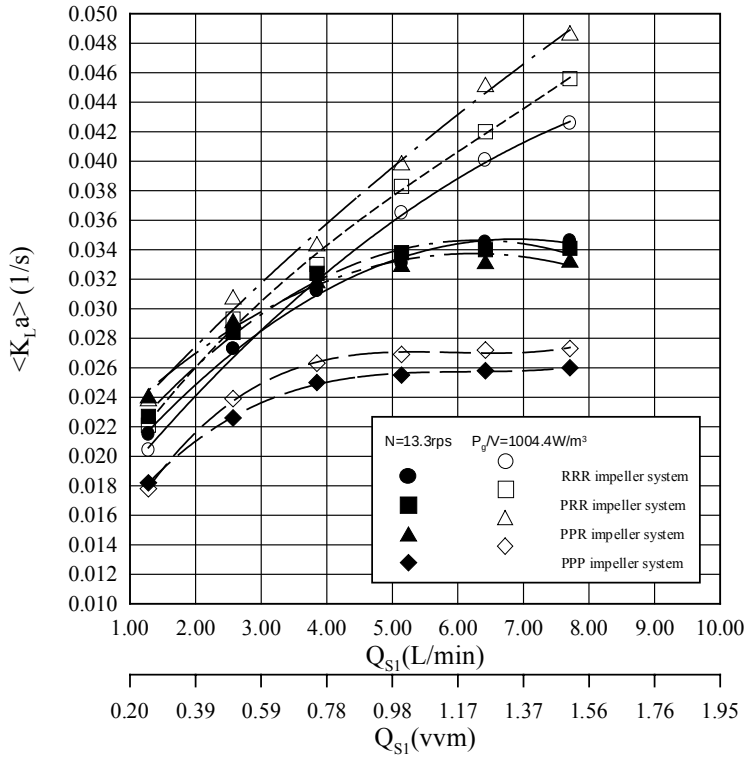

Fig. 8.4-5 The plots of $<K_La>$ and Q_S for the *RRR*, *PRR*, *PPR* and *PPP* systems with *N=13.3 rps* as well as P_g/V=1004.4 W/m^3.

Figure 8.4-5 shows the plot of $<K_La>$ vs. the original sparged gas rate to the lowest impeller of each system, i.e., Q_{S1} for the RRR, PRR, PPR and PPP impeller systems with the same rotational speed N=13.3rps as well as the same energy dissipation density P_g/V=1004.4W/m^3. For a given rotational speed, regardless of the impeller combinations, the $<K_La>$ values increase with the increase in aeration rate until the flooding point of the lowest impellers are reached and leveling-off values of $<K_La>$ are attainable. Under a gas completely dispersed condition, the PRR and PPR systems give higher values of $<K_La>$ than the RRR system due to the larger circulation flow provided by the pitched blade impeller. However, if the sparged gas rate exceeds a certain value (Q_{S1}>6.5L/min=1.25vvm) or near the flooding condition, the RRR system has the highest value of $<K_La>$ due to the better gas dispersion capabilities of the upper Rushton turbine impellers than those for the upper-pitched blade impellers in other systems. To have the same P_g/V for each system, the rotational speeds of the PRR and PPR systems should be increased to larger values than that for the RRR system. As a result, the PRR and PPR systems provide larger pumping rates and better gas dispersions than the RRR system, which induces the PPR system gives the highest $<K_La>$ among these systems. Increasing the rotational speed of each impeller to give the same P_g/V value for each impeller system, the flooding points of the lower impeller impellers in each impeller

combination has shifted to higher aeration rates. It makes the $<K_La>$ values increase monotonically with the increase in aeration rate, except for the PPP system. It is worthy to note that regardless of operating conditions, the PPP system always gives much smaller $<K_La>$ than those of the other three systems due to the insufficient gas dispersion of the lowest pitched blade impeller.

From the above results, one may recognize that the PPR system may be the best design among these four systems since it gives the largest $<K_La>$. However, from the results shown in Fig. 8.4-4, it is found that the largest local mass transfer coefficients around the Rushton turbine impeller are as larger as 1.5 times of those around the pitched blade impellers. This fact indicates that if a high $<K_La>$ environment is desired for process requirement, the RRR system may still be the most appropriate design among these impeller systems.

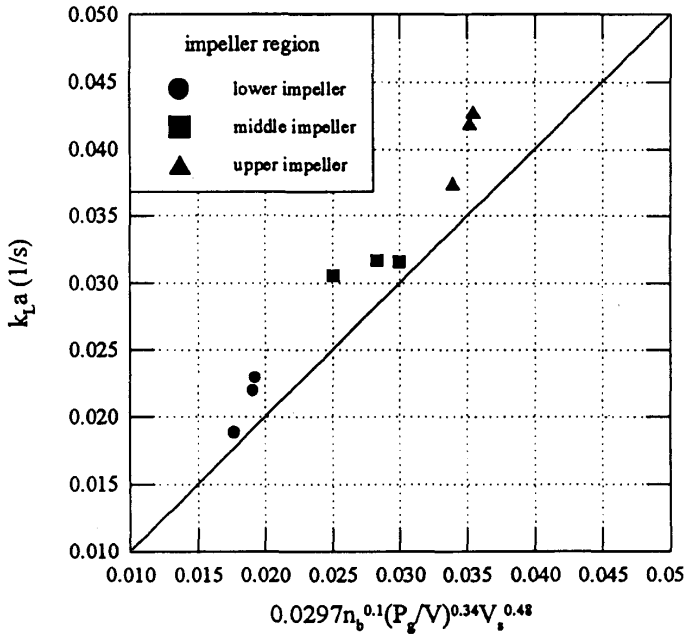

Fig. 8.4-6 Applicability of $<K_La>$ correlation for the single impeller systems to the multi-impeller system.

8.4.4 Applicability of the $<K_La>$ correlation of the single impeller system to the multiple impeller systems

To examine whether Eq.(8.2-3), resulting from the single impeller system, can be applied to multiple impeller systems, the K_La data obtainec from the triple impeller system is plotted vs. $0.0297n_b^{0.1}(P_g/V)^{0.34}V_s^{0.48}$ in Fig.8.4-6. The results shown in this figure indicate that although the deviation among the correlation and the data are not so close, it still can be applied to estimate $<K_La>$ values for each impeller region of the multipleimpeller systems. To confirm this viewpoint further, the experimental K_La values obtained from the single six blades impeller were correlated as

$$\langle K_L a \rangle = 0.046\left(P_g/V\right)^{0.53} V_s^{0.52} \tag{8.4-5}$$

the deviation of this correlation is less than 3%. Fig. 8.4-7 show the comparison of K_La value for each impeller system with Eq. (8.4-5). The result shown in this figure clearly indicateds that the behavior of each impeller in any multiple impeller system under gassing condition is identical as long as the net energy dissipation density, P_g/V, and its superficial gas velocity of gas, V_S, are the same.

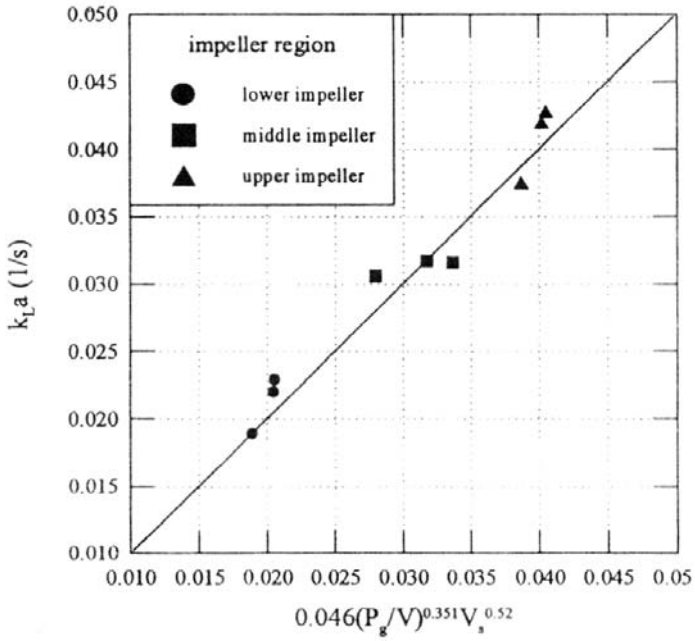

Fig. 8.4-7 Applicability of Eq. (8.4-5) to multiple impeller systems.

8.4.5 Relationship between the Power Consumption and Mass Transfer Rate

Since K_La is closely related to turbulent intensity as well as the relative velocity between different phases, it is very interesting to examine the relationship between power drawn and the average mass transfer coefficient around each impeller. Table 8.4-5 lists the experimentally determined power drawn data and average mass transfer coefficient around each impeller $\langle K_La \rangle_D$ for various impeller combinations under the same rotational speed (N=13.3rps) as well as the same energy dissipation density (P_g/V=1004.4W/m^3) with Q_{S1}=2.57L/min=0.5vvm. From the plot of $\langle K_La \rangle_D$ vs. P_g/V for each impeller shown in Fig.8.4-8, it is found that the data points can be divided into two categories, i.e. the systems with at least a Rushton turbine impeller and system without the Rushton turbine impeller. In each group, if impellers draw the same quantity of power, each impeller will give similar average mass transfer rate and all data points settle at two different straight lines. Even the PPP system gives a much stronger liquid circulating flow than the other systems with a given P_g/V, the worse gas dispersion capability of the lowest pitched blade impeller makes the PPP

system give a much smaller <$K_L a$>. The difference in the capability of gas dispersion between the pitched blade impeller and Rushton turbine impeller enlarges with the increase in power consumption. This fact induces the size of dispersed bubbles given by the pitched blade impeller larger than those generated by the Rushton turbine impeller, which causes the PPP system give a much smaller <$K_L a$>. From the above results, one may conclude that the impeller with a better gas dispersion capability, such as Rushton turbine impeller, should be adopted as the lowest impeller for the multiple impeller gas-liquid contactors.

Table 8.4-5 Comparisons of the power drawn by each impeller for various impeller combinations with constant *N* as well as the same P_g/V under Q_S=0.5vvm=2.57L/min. (*referential system).

Operational condition	System / Impeller	RRR*			PRR			PPR			PPP		
		P_g/V (W/m^3)	Power Ratio	<$K_L a$>$_D$	P_g/V (W/m^3)	Power Ratio	<$K_L a$>$_D$	P_g/V (W/m^3)	Power Ratio	<$K_L a$>$_D$	P_g/V (W/m^3)	Power Ratio	<$K_L a$>$_D$
N=13.3rps	Uppest impeller	363.6	1.27	0.033	182.2	0.64	0.024	192.3	0.64	0.025	165.9	0.58	0.025
	Middle impeller	355.6	1.25	0.032	337.3	1.18	0.033	197.5	0.69	0.025	162.2	0.57	0.025
	Lowest impeller	285.2	1.00	0.031	305.5	1.07	0.032	302.4	1.06	0.034	141.9	0.50	0.023
	<$K_L a$>	0.027			0.028			0.029			0.023		
P_g/V=1004.4W/m^3	Uppest impeller	363.6	1.27	0.033	210.0	0.74	0.024	239.9	0.84	0.027	352.5	1.24	0.027
	Middle impeller	355.6	1.25	0.032	403.1	1.41	0.036	241.9	0.85	0.027	344.5	1.21	0.027
	Lowest impeller	285.2	1.00	0.031	391.3	1.37	0.035	522.6	1.83	0.040	307.3	1.08	0.026
	<$K_L a$>	0.027			0.029			0.031			0.024		

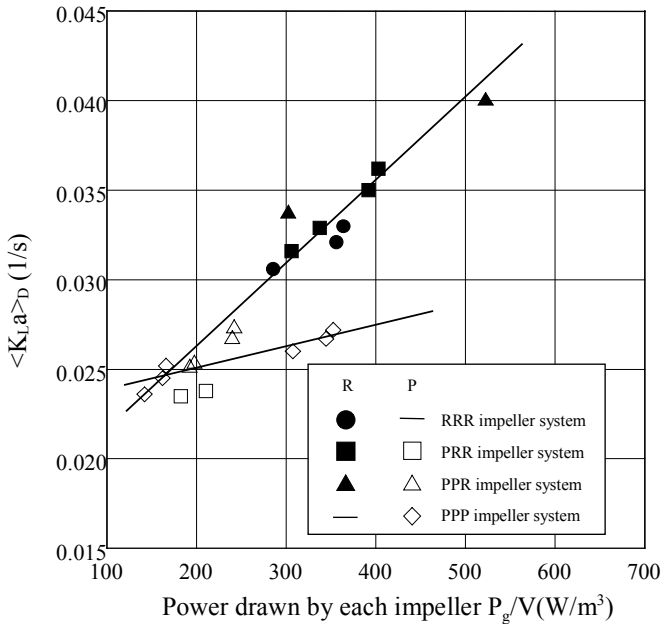

Fig. 8.4-8 Relationship between the power drawn by each impeller and the average mass transfer coefficient around each impeller with Q_S=0.5vvm.

8.5 Estimation of $\langle K_L a \rangle_D$ around Each Impeller in Multiple Impeller Systems

To examine whether the data obtained in this study can be fitted to the correlations published in the literature, the overall average $\langle K_L a \rangle$ values for various multiple impeller systems obtained in this study are plotted in Fig.8.5-1 along with several correlations proposed by previous researchers. From the results shown in this figure, it is found that no single previous correlation is able to fit all mass transfer data, and only the Linek's correlation fits our data obtained in the RRR system with a higher level of energy dissipation density.

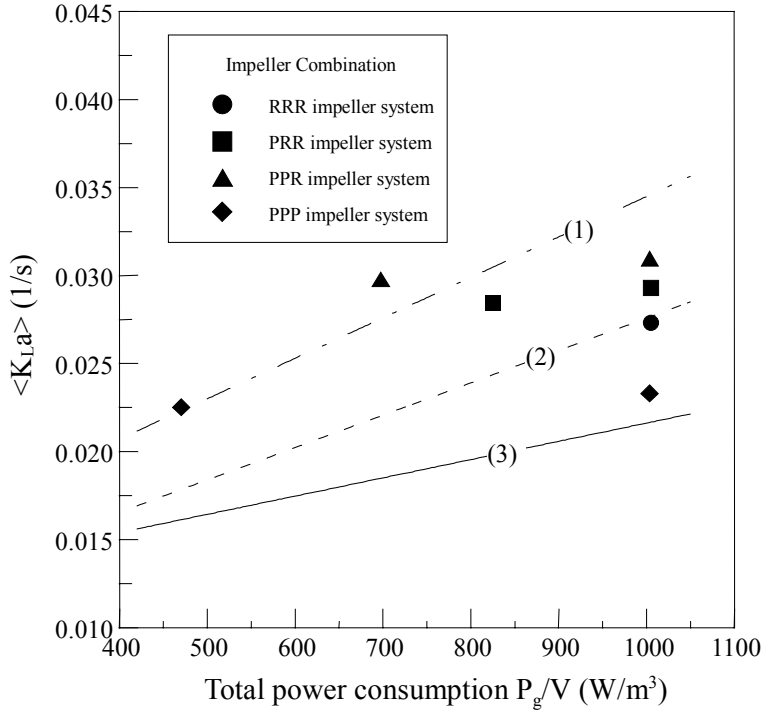

(1) Nocentini et al.(1993) $1.5\times10^{-2}\,(P_g/V)^{0.59}\,(V_S)^{0.55}$

(2) Linek et al. (1987) $4.95\times10^{-3}\,(P_g/V)^{0.59}\,(V_S)^{0.4}$

(3) Van't Riet (1979) $2.6\times10^{-2}\,(P_g/V)^{0.4}\,(V_S)^{0.5}$

Fig. 8.5-1 Comparison of various correlations of $\langle K_L a \rangle$ for multiple impeller systems with the experimental data.

From the discussions seen in above sections, it is known that the recirculated gas plays a very important role in both the energy dissipation and the mass transfer rate around each impeller. As shown in chap. 5, two straight lines are enough to display the relation between $(P_g/P_o)_n$ and N_A', while a more complicated curve is needed to fit the relationship between $(P_g/P_o)_n$ and N_A under the same situation. This result indicated that the modified aeration number $N_A'(=Q_t/ND^3)$ is more appropriate than the aeration number $N_A(=Q_{S1}/ND^3)$, based on the sparged gas rate Q_{S1} only, to relate the power drawn (P_g/P_o) by the impeller. Therefore, it is interesting to examine the relation between $\langle K_L a \rangle_D$ and N_A'. The authors (Lu et al., 2000) had

studied the mass transfer performances in single impeller systems and found that a straight line based on the modified aeration number N_A' was enough to correlate the averaged mass transfer coefficient around the impeller $<K_La>_D$ and the correlation was given as:

$$<K_La>_D=0.134\ (Q_t/ND^3) + 0.00339 \qquad (8.5\text{-}1)$$

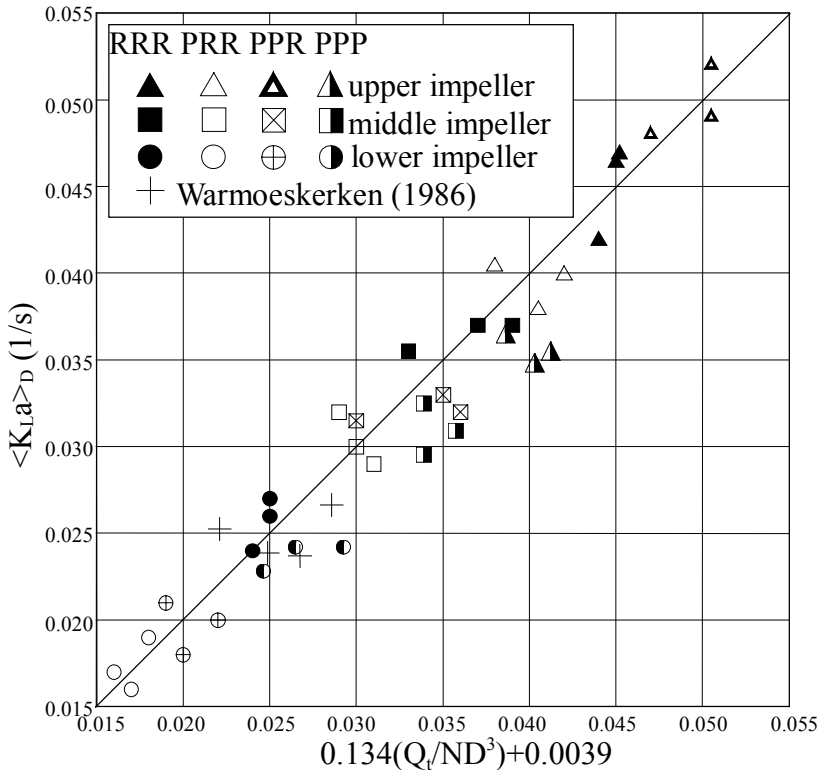

Fig. 8.5-2 The plots of Eq.(8.5-1) and available experimental date for $<K_La>_D$ along with the $<K_La>$ provided by Warmoeskerken (1986).

To see whether Eq. (8.5-1) is applicable to each impeller in multiple impeller systems, the K_La data were recalculated to obtain $<K_La>_D$ and the results are plotted against $0.134\ (Q_{tn}/ND^3) + 0.00339$ in Fig.8.5-2 along with the $<K_La>_D$ provided by Warmoeskerken (1986) for the single Rushton turbine impeller system. Where Q_{tn} was the total gassing rate around each impeller, equal to the sum of Q_{Sn} and Q_{Rn} as shown in in Chap.5. The values of Q_{tn} for the data of Warmoeskerken (1986) were calculated from the above correlations based on the value of N_A provided by him. From the plot shown in Fig.8.5-2, it is clearly found that all the experimental $<K_La>_D$ data obtained in this study and the data provided by Warmoeskerken (1986) for single impeller system settle around a single straight line, and the deviations are less than 15%. This result indicates that Eq. (8.5-1) can be applied not only to single impeller systems, but also to each impeller in any multiple Impeller system as well. In order to evaluate the overall average mass transfer coefficient $<K_La>$ for the systems equipped with

different impeller combinations through Eq.(8.5-1), it is necessary to relate $<K_La>$ to $<K_La>_D$. From the measured local K_La data, the values of $<K_La>$ and $<K_La>_D$ were recalculated as shown in Table 8.4-5, and the relationship between $<K_La>$ and $<K_{La}>_D$ were proposed for different impeller combination systems as:

$$< K_L a >= \frac{1}{3}\left[0.85\left(< K_L a >_{DL} + < K_L a >_{DM} + < K_L a >_{DU}\right)\right] \quad \text{for RRR system (8.5-2)}$$

$$< K_L a >= \frac{1}{3}\left[1.3 < K_L a >_{DL} + 0.9 \times 0.85 < K_L a >_{DM} + 0.85 < K_L a >_{DU}\right] \quad \text{for PPR system (8.5-3)}$$

$$< K_L a >= \frac{1}{3}\left[1.3 < K_L a >_{DL} + 1.3 < K_L a >_{DM} + 0.7 \times 0.85 < K_L a >_{DU}\right] \quad \text{for PPR system (8.5-4)}$$

$$< K_L a >= 0.91\left[\frac{1}{3}\left(< K_L a >_{DL} + < K_L a >_{DM} + < K_L a >_{DU}\right)\right] \quad \text{for PPP system (8.5-5)}$$

By combining Eq.(8.5-1) with Eqs.(8.5-2)-(8.5-5), the overall average mass transfer coefficients for various multiple impeller combination systems can be estimated.

NOTATION

a	Gas-liquid interface area per unit volume	[1/m]
B	Baffle width	[m]
C	Distance between impeller	[m]
D	Impeller diameter	[m]
H	Liquid height of stirred tank	[m]
h_0	Distance between tank bottom and the lowest impeller	[m]
k_L^0	Mass transfer coefficient	[m/hr]
K_G	Gas side mass transfer coefficient	[m/s]
K_L	Liquid side mass transfer coefficient	[m/s]
K_La	Local mass transfer coefficient at measuring point	[1/s]
$<K_La>$	Overall volume-average mass transfer coefficient of the whole vessel	[1/s]
$<K_La>_D$	Volume-average mass transfer coefficient around each impeller	[1/s]
n_b	Impeller blade number	[-]
n_s	The stage of the impeller(>1)	[-]
N	Impeller rotational speed	[1/s]
N_A	Aeration number($=Q_s/ND^3$)	[-]
N_A'	The modified aeration number ($=Q_t/ND^3$)	[-]
Np	Power number	[-]
$\boldsymbol{P(c, \theta)}$	Probability density function of concentration	[-]
P,p	Power	[HP]
P_0	Ungassed impeller power consumption	[HP]
P_g	Power consumption under aeration	[HP]

P_o	Power consumption without aeration	[HP]
P_v	Power consumption per unit volume	[HP/m^3]
Q_s	Sparged gas flow rate	[m^3/s]
S	Overall interfacial area	[m^2]
T	Tank diameter	[m]
t	Time	[hr]
<u'>	Volume-averaged turbulent fluctuating velocity	[m/s]
u'	Velocity fluctuation	[m/s]
V	Liquid volume in the tank	[m^3]
V_s	Superficial gas velocity	[m/s]
vvm	The ratio of aeration rate per minute /the liquid volume in the tank	[1/s]
w	Impeller blade width	[m]

<*Greeks Letters*>

β	Mixing intensity	[1/s]
ε	Energy dispersion per unit mass of fluid	[m^2/s^2]
η	Efficiency of mixing power	[-]
θ	Time	[s][hr]
ρ	Liquid density	[kg/m^3]
σ^2	Variance of concentration distribution	[g^2/l^2]
ω	Mean rotation rate	[1/s]

<*Subscripts*>

A	Component A(Oxygen)
B	Component B(Sulphite)
f	Final condition
g	Gassed condition
n	The n^{th} stage of the impeller
o	Initial condition

<*Superscripts*>

*	Saturated solubility of gaseous component at the gas-liquid interface
-	Average quantity

<*Abbreviation*>

PPP	The system equipped with three pitched blade impellers
PPR	The system equipped with a lower Rushton turbine impeller and two upper pitched blade impellers
PRR	The system equipped with two lower Rushton turbine impeller and a upper Pitched blade impellers
RRR	The system equipped with three Rushton turbine impellers